Research Article

Triple diffusive convection with Soret–Dufour effects in a Maxwell nanofluid saturated in a Darcy porous medium

Reema Singh[1] · Jaimala Bishnoi[1] · Vipin Kumar Tyagi[2]

Received: 12 January 2020 / Accepted: 10 March 2020 / Published online: 19 March 2020

Abstract
Soret–Dufour phenomenon in a Darcy–Maxwell Brownian nanofluid is performed using a macroscopic filtration model, suggested by Alishayev (Hydromechanics 3:166–174, 1974). For nanoparticle flux at the boundaries passive management, influenced by the management of concentration flux assumed in Stefan's flow, is considered. Normal mode technique is used to analyse the stationary and oscillatory convections under the linear stability theory. The effects of different phenomenon are quantified by dimensionless parameters. It is found that the Soret parameter has dual behaviour for stationary convection and destabilizing behaviour for oscillatory convection, whereas the Dufour parameter has a stabilizing effect for both stationary and oscillatory convections. Nonlinear stability analysis provides the behaviour of flux of heat, salt and nanoparticles in the flow field through Nu, Nu_C and Nu_ϕ. Steady and unsteady convections are discussed. A graphical representation of streamlines, isotherms, isohalines and flow lines of nanoparticles concentrations is presented.

Keywords Darcy–Maxwell nanofluid · Soret–Dufour-driven convection · Linear and nonlinear instability · Passive management of nanoparticle at the boundaries

List of symbols

c	Nanofluid specific heat at constant pressure
C^*	Solute concentration
C	Dimensionless temperature
C_c^*	Concentration at the upper wall
C_h^*	Concentration at the lower wall
$(\rho c)_m$	Effective heat capacity of the medium
$(\rho c)_f$	Effective heat capacity of the fluid
$(\rho c)_p$	Effective heat capacity of the material constituting nanoparticles
D_B	Brownian diffusion coefficient
D_T	Thermophoretic diffusion coefficient
D_S	Diffusion coefficient
d	Dimensional layer depth
$\boldsymbol{g}$	Gravitational acceleration vector
K	Permeability of the porous medium
Le	Thermosolutal Lewis number
Ln	Thermo-nanofluid Lewis number
N_A	Modified diffusivity ratio
N_B	Modified particle density increment
N_{CT}	Soret parameter
N_{TC}	Dufour parameter
p^*	Pressure
p	Dimensionless pressure
Ra	Thermal Rayleigh–Darcy number
Rm	Basic density Rayleigh–Darcy number
Rn	Concentration Rayleigh–Darcy number
Rs	Solutal Rayleigh number
t^*	Time
t	Dimensionless time
T^*	Temperature
T	Dimensionless temperature
T_c^*	Temperature at the upper wall
T_h^*	Temperature at the lower wall
(x^*, y^*, z^*)	Cartesian coordinates
(x, y, z)	Dimensionless Cartesian coordinates

✉ Reema Singh, reemamalik28@gmail.com; Jaimala Bishnoi, jaimalaccsu1@gmail.com; Vipin Kumar Tyagi, prvipin22@gmail.com | [1]Department of Mathematics, Chaudhary Charan Singh University, Meerut, UP 250004, India. [2]SBAS, Shobhit Deemed University, Meerut, UP 250110, India.

SN Applied Sciences (2020) 2:704 | https://doi.org/10.1007/s42452-020-2462-4

$\mathbf{v}$	Nanofluid velocity
$\mathbf{v}_D^*$	Darcian velocity ($=\varepsilon\mathbf{v}$)
$\mathbf{v}_D$	Dimensionless Darcy velocity

Greek symbols

κ	Thermal conductivity of the nanofluid
κ_m	Effective thermal conductivity of the porous medium
α_m	Thermal diffusivity of the porous medium
β_T	Thermal volumetric coefficient
β_C	Solutal volumetric coefficient
σ	Heat capacity ratio
ε	Porosity
μ	Viscosity of the fluid
λ	Relaxation time
ρ	Fluid density
ρ_p	Nanoparticle mass density
ϕ^*	Nanoparticle volume fraction
ϕ_0^*	Reference value of nanoparticle volume fraction
ϕ	Dimensionless nanoparticle volume fraction
α	Wave number
ω	Frequency of oscillations
ψ	Stream function

Subscripts

b	Basic solution

Superscripts

*	Dimensional variable
′	Perturbation variable

Operators

∇^2	$\frac{\partial^2}{\partial x^2}+\frac{\partial^2}{\partial y^2}+\frac{\partial^2}{\partial z^2}$
∇_1^2	$\frac{\partial^2}{\partial x^2}+\frac{\partial^2}{\partial z^2}$

1 Introduction

To meet the technical challenges of increased heat loads, heat fluxes and pressure drops in the field of photonics, microelectronics, metrology, optoelectronics, power manufacturing, defence and transportation, nanofluids prove to be one of the most promising, exciting and novel class of nanotechnology-based heat transfer fluids. Remarkable researches on different types of nanofluids, establishing these as next-generation smart fluids, have been documented by Eastman et al. [2], Das et al. [3], Bianco et al. [4] and Nield and Bejan [5].

Nanofluids introduced by Choi et al. [6] are two-phase mixtures composed of nanosized fine particles or fibres suspended in the continuous and saturated liquids. In nanofluids, migration of nanoparticles is a quintessential mechanism affecting the coefficient of convective heat transfer and pressure drop and, therefore, serves as an interesting alternative for advanced thermal applications. Buongiorno [7] made an attempt to include the effect of nanoparticle migration in nanofluids and obtained more realistic results. He considered a dilute mixture of nanoparticles in an incompressible base fluid with heat transfer subjected to thermal equilibrium between nanoparticles and base fluid. It was assumed that chemical reactions are absent, and external forces, viscous dissipation and radiative heat transfer are negligible. He suggested the conservation equation for nanoparticles as

$$\frac{\partial\phi^*}{\partial t^*}+\mathbf{v}^*\cdot\nabla^*\phi^*=\nabla^*\cdot\left[D_B\nabla^*\phi^*+(D_T/T_c^*)\nabla^*T^*\right], \tag{1}$$

where ϕ^* is the volume fraction, $\mathbf{v}^*$ is the velocity, D_B is the Brownian coefficient and D_T is the thermophoretic diffusion coefficient.

In Eq. (1), the second term on the left-hand side states that nanoparticles move homogeneously with the fluid and the terms on the right-hand side predict that the nanoparticles simultaneously have a slip velocity relative to the fluid due to Brownian diffusion and thermophoresis where the second term contributes to the migration of nanoparticles due to temperature.

In natural convection of nanofluids, these slip mechanisms do not allow the nanoparticles to accompany fluid molecules, resulting in a non-uniform distribution of the volume fraction of nanofluids and consecutively creating a variable concentration of nanoparticles in a mixture. The variability of concentration of nanoparticles induces the Dufour effect accommodated in the energy equation as follows:

$$(\rho c)_p\left(\frac{\partial T^*}{\partial t^*}+\mathbf{v}^*\cdot\nabla^*T^*\right)=\kappa\nabla^{*2}T^*+(\rho c)_p\left[D_B\nabla^*\phi^*\cdot\nabla^*T^*+(D_T/T_c^*)\nabla^*T^*\cdot\nabla^*T^*\right], \tag{2}$$

where Eq. (2) shows that heat may be transported via convection (second term on the left-hand side), via conduction (first term on the right-hand side), and simultaneously via virtue of nanoparticle migration (second and third terms on the right-hand side). In fact, Buongiorno's model states that there are thermo-diffusion and diffusion-thermo effects in nanofluids and hence an anomalous convective heat transfer is reported. Buongiorno's model plays an incredible role for various researches on different aspects of nanofluids [5, 8–15].

Double diffusive convection, first recognized in the late 1950s, has established its importance in the fields as diverse as geophysics, astrophysics, metallurgy, chemistry and obviously in the parent field—ocean physics [5, 16]. Exponential research on double diffusive convection in nanofluids is continuously portraying the binary nanofluids as working fluids in the various fields.

Chamkha et al. [17] presented the numerical as well as analytical solutions in a vertical channel for micropolar fluid. Thermosolutal Marangoni convection flow of an electrically conducting fluid along a vertical surface with magnetic field, heat generation or absorption investigated by Al-Mudhaf and Chamkha [18]. Using Brinkman–Forchheimer-extended Darcy equations, numerical study of mixed convection in a vertical porous channel proposed by Umavathi et al. [19]. Further thermosolutal study for MHD Marangoni boundary layers problem discussed by Magyari and Chamkha [20]. Khedr et al. [21] presented the steady, laminar, MHD flow of a micropolar fluid in the presence of magnetic field, thermal radiation effects and heat generation/absorption phenomenon. Further, Magyari and Chamkha [22] given the full analytical solution for micropolar fluid in the presence of heat generation or absorption over a uniformly stretched permeable surface. In addition, Chamkha et al. [23] investigated the unsteady MHD natural convection with Joule heating, chemical reaction and radiation effects of micropolar fluid.

In a convective system also, where the motions of conventional binary liquids and gases are governed by buoyancy, induced by density differences in the constituents and not suffered by the internal dissipative effects like viscous friction and diffusion, the temperature and concentration are not independent rather coupled via thermo-diffusion and diffusion-thermo mechanism. Such a coupled mechanism in chemically non-reacting and miscible binary mixtures is important in bifurcation theory and structure formation.

For the first time, diffusion-thermo phenomenon was observed in 1873 by the Swiss physicist Dufour [24]. He noticed that if two chemically different non-reacting gases or liquids, which were initially at the same temperature, were allowed to diffuse into each other, then a difference of temperatures in the system occurred and the difference was retained if a concentration gradient was maintained. In gases, the difference can reach several degrees (for example, for nitrogen with hydrogen it measures approximately 10^3 °C). Ingle and Horne [25] mentioned that the effect is of interest in liquids for three important reasons: (1) it can be used to verify the heat matter Onsager reciprocal relation, (2) the temperature variations could cause complications in diffusion experiments, and (3) it has never been unambiguously observed. In 1879, a reverse phenomenon of thermo-diffusion in liquids was observed by another Swiss Scientist Soret [26]. He performed an experiment with sodium chloride and potassium nitrate in a tube by maintaining the top at 800 °C and the bottom end of it at room temperature and noticed that in direct diffusion in isotropic fluid systems the concentration gradient is induced by the driving force of applied temperature gradient until the system reaches the steady-state condition. De Groot and Mazur [27] explained the Soret and Dufour effects and elaborated the conservation equations for concentration and energy accommodating the Soret and Dufour parameters.

Soret and Dufour effects, being considered as second-order phenomena on the basis that they are of smaller order of magnitude than the effects described by Fourier's and Fick's laws for energy transport and mass transport, respectively, are often neglected. It is a general view that in liquid mixtures Soret effect dominates and Dufour effect is negligible, while in gaseous mixtures the Dufour coupling becomes more and more important and can change the stability behaviour significantly in comparison with liquid mixtures. But there are exceptions; Eckert and Drake [28], Nithyadevi and Yang [29] and Weaver and Viskanta [30] discovered several cases where the Soret and/or Dufour effects cannot be ignored. These effects are often encountered in chemical process engineering, in the area of reactor safety, in combustion flames, in high-speed aerodynamics, in oceanography, in solar collectors and in various porous flow regimes occurring in geophysical systems [25, 28]. Ryskin et al. [31] considered the Soret effect in ferromagnetic nanofluid and showed that nanoparticles inhibit the stability of the system in comparison with the conventional fluid. Kim et al. [32, 33] and Kim and Choi [34] studied the thermo-diffusion and diffusion-thermo effects on convective instabilities of Newtonian nanofluid. They concluded that both the Soret and Dufour effects make nanofluid unstable, and the transfer of heat is enhanced in a significant amount.

With reference to the heat and mass transfer, a physically realistic phenomenon is suggested by Stefan, i.e. flux of concentration cannot be adjusted at the boundaries rather it is zero there [35]. This phenomenon is equally valid in nanofluids. Nanoparticle volumetric fraction cannot be adjusted at the boundaries, and therefore, there will be no flux of nanoparticles over there. Nield and Kuznetsov [36] discussed the thermal instability of a nanofluid-saturated porous medium incorporating the phenomenon of passive management of nanoparticles and assumed no flux of them at the boundaries. Following them, many problems have been investigated under passive management of nanoparticles at the boundaries and others already done for active management have been revised or reinvestigated.

The phenomenological model for the low Reynold number Maxwell fluid suggested by Alishayev [1] and generalized as the macroscopic filtration model by Khuzayorov et al. [37] is valid for a dense porous medium of sufficiently large thickness. Few research papers on double diffusive convection using this model are reported in the literature. Linear stability of double diffusive convection has been presented by Wang and Tan [38]. Awad et al. [39] extended

the work for cross-diffusion effects. They considered viscous variations in the model suggested by Brinkman and showed that the relaxation time and the Soret parameter destabilize the system, while Dufour parameter stabilizes it. Wang and Tan [40] analysed the linear and nonlinear stability of Soret-driven convection and showed that the relaxation parameter is responsible for decreasing the heat transfer rate, while it increases with increasing the Soret parameter (negative or positive). Malashetty and Biradar [41] considered velocity variations in the model to discuss the cross-diffusion effects. Some of the important results obtained by them are that Dufour coefficient advances the oscillatory convection, negative Soret coefficient stabilizes the stationary convection and positive Soret convection destabilizes it. Jaimala and Goyal [42] investigated the thermosolutal convection with cross-diffusion effects under linear stability theory. Narayana et al. [43] widened the domain of the work presented by Wang and Tan [40] by incorporating the Dufour effect. They showed that the stationary and oscillatory convections may not occur simultaneously. They showed that the Soret effect is to reduce the heat transport and to increase the mass transport, while the Dufour parameter produces the reverse effects on the two transports. Zhao et al. [44] considered the modified Darcy–Maxwell model [1] to discuss the triply diffusive convection driven by three agencies: heat and two types of salts having different diffusive properties. They have ignored the cross-diffusion effects. Recently, Chand and Rana [45] discussed the cross-diffusion effects under the linear stability theory by considering Darcy–Maxwell fluid layer in which heat as well as salt is greater on lower plate comparative to upper one.

Recognizing various important applications of nanofluids, the objective of the present paper is to use Alishayev model [1] to investigate the double diffusive convection of Darcy–Maxwell nanofluid with cross-diffusion effects introduced through two pairs of agencies in nanofluids (heat and nanoparticles and heat and salt). We confine ourselves to the zero flux of nanoparticles at the boundaries. To find the behaviour of different parameters in the presence of nanoparticles, a comparison has been made with Narayana et al. [43] and Chand and Rana [45], the work dedicated to the convection in a Maxwell fluid with no nanoparticles.

2 Physical model and mathematical analysis

We consider an incompressible Maxwell viscoelastic nanofluid layer in a Darcy porous medium, which is infinitely extended in x- and y-directions. The porous layer is isotropic and confined between two impermeable parallel planes such that the lower plane is situated at $z = 0$, whereas the upper plane is situated at $z = d$. T_h^*, C_h^* and T_c^*, C_c^* are the temperatures and solute concentrations at the lower and upper planes, respectively, such that $T_h^* > T_c^*$ and $C_h^* > C_c^*$. This system is shown in schematic form in Fig. 1. It is assumed that nanoparticles and base fluid are in local thermal equilibrium. Following Bungiorno [7] external forces, chemical reaction, viscous dissipation and radiative heat transfer are negligible and particle-related effects like particle inertia, Magnus effects, etc., have also not been considered.

Following Alishayev [1], Eastman et al. [2], Buongiorno [7] and Nield and Kuznetsov [36], continuity equation, momentum equation, thermal energy equation, solute concentration equation and nanoparticle concentration equation, in dimensional form, are taken as

$$\nabla^* \cdot \mathbf{v}_D^* = 0, \tag{3}$$

$$\frac{\mu}{K}\mathbf{v}_D^* = \left(1 + \lambda^* \frac{\partial}{\partial t^*}\right)\left[-\nabla^* p^* + \left[\phi^* \rho_p + (1-\phi^*)\left\{\rho\left\langle 1 - \beta_T(T^* - T_c^*) - \beta_C\left(C^* - C_c^*\right)\right\rangle\right\}\right]\boldsymbol{g}\right], \tag{4}$$

$$(\rho c)_m \frac{\partial T^*}{\partial t^*} + (\rho c)_f \mathbf{v}_D^* \cdot \nabla^* T^* = \kappa_m \nabla^{*2} T^* + \varepsilon(\rho c)_p \left[D_B \nabla^* \phi^* \cdot \nabla^* T^* + (D_T/T_c^*)\nabla^* T^* \cdot \nabla^* T^*\right] + (\rho c)_f D_{TC} \nabla^{*2} C^*, \tag{5}$$

$$\frac{\partial C^*}{\partial t^*} + \frac{1}{\varepsilon}\mathbf{v}_D^* \cdot \nabla^* C^* = D_{Sm} \nabla^{*2} C^* + D_{CT} \nabla^{*2} T^*, \tag{6}$$

$$\frac{\partial \phi^*}{\partial t^*} + \frac{1}{\varepsilon}\mathbf{v}_D^* \cdot \nabla^* \phi^* = D_B \nabla^{*2} \phi^* + (D_T/T_c^*)\nabla^{*2} T^*, \tag{7}$$

where $\mathbf{v}_D^* = (u^*, v^*, w^*)$ is the Eulerian Darcy velocity, μ is the Darcian viscosity, p^* is the pressure, K is the permeability, ϕ^* is the nanoparticle concentration, t^* is the time, λ^* is the relaxation time, ρ is the density of the base fluid, ρ_p is the mass density of nanoparticles, β_T and β_C are the

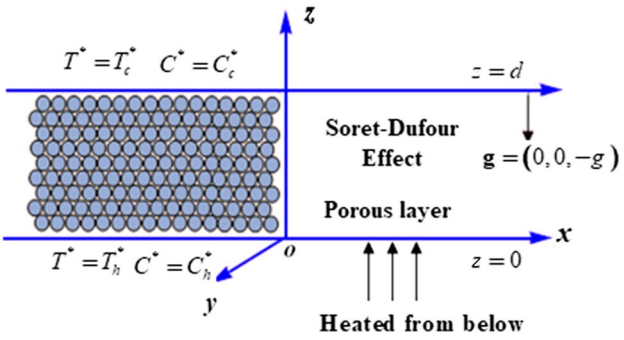

Fig. 1 Physical configuration of the problem

coefficients of thermal and solutal expansions, respectively, T_c^* is the reference temperature, C_c^* is the reference solutal concentration, g is the gravitational acceleration in the negative z-direction, c is the specific heat of nanofluid at constant pressure, κ is the thermal conductivity of the fluid, κ_m is the effective thermal conductivity of the porous medium and is equal to $\varepsilon\kappa$, $(\rho c)_m$, $(\rho c)_f$ and $(\rho c)_p$ are the effective heat capacity of the medium, the fluid and the material constituting nanoparticles, ε is the porosity, D_{Sm} is the diffusion coefficient of salt, D_{TC} is the Dufour coefficient and D_{CT} is the Soret coefficient of salt, D_B is the Brownian diffusion coefficient and D_T is the thermophoretic diffusion coefficient.

$$\mathrm{Ra} = \frac{\rho g \beta K d (T_h^* - T_c^*)}{\mu \alpha_m} \quad \text{(thermal Rayleigh–Darcy number)},$$

$$\mathrm{Rn} = \frac{\phi_0^* g K d (\rho_p - \rho)}{\mu \alpha_m} \quad \text{(concentration Rayleigh–Darcy number)},$$

$$\mathrm{Rm} = \frac{gKd\left[\rho_p \phi_0^* + \rho(1-\phi_0^*)\right]}{\mu \alpha_m} \quad \text{(basic density Rayleigh–Darcy number)},$$

$$\mathrm{Rs} = \frac{\rho g K d \beta_C \left(C_h^* - C_c^*\right)}{\mu D_S} \quad \text{(solutal Rayleigh–Darcy number)},$$

$$N_A = \frac{D_T (T_h^* - T_c^*)}{D_B T_c^* \phi_0^*} \quad \text{(modified diffusivity ratio)},$$

$$N_B = \frac{\varepsilon \phi_0^* (\rho c)_p}{(\rho c)_f} \quad \text{(modified particle density increment)},$$

$$\mathrm{Le} = \frac{\alpha_m}{D_B} \quad \text{(thermo-nanofluid Lewis number)},$$

$$\mathrm{Ln} = \frac{\alpha_m}{D_S} \quad \text{(thermo-solutal Lewis number)},$$

$$N_{TC} = \frac{D_{TC}(C_h^* - C_c^*)}{(T_h^* - T_c^*)} \quad \text{(Dufour parameter)}$$

and $N_{CT} = \frac{D_{CT}(T_h^* - T_c^*)}{(C_h^* - C_c^*)}$ (Soret parameter).

Here, $\alpha_m = \frac{\kappa_m}{(\rho c)_f}$ is the thermal diffusivity of the porous medium and $\sigma = \frac{(\rho c)_m}{(\rho c)_f}$.

In analogy with the Stephan's flow [32], it is assumed that at the boundaries, the flux of nanoparticles is zero [33]. Thus, the boundary conditions are considered as

$$\mathbf{v}_D^* = 0,\ T^* = T_h^*,\ C^* = C_h^*,\ D_B \frac{\partial \phi^*}{\partial z^*} + \frac{D_T}{T_c^*} \frac{\partial T^*}{\partial z^*} = 0 \text{ at } z = 0, \tag{8}$$

$$\mathbf{v}_D^* = 0,\ T^* = T_c^*,\ C^* = C_c^*,\ D_B \frac{\partial \phi^*}{\partial z^*} + \frac{D_T}{T_c^*} \frac{\partial T^*}{\partial z^*} = 0 \text{ at } z = d. \tag{9}$$

Following Singh et al. [46], under linear stability analysis, the Galerkin-type weighted residual method has been used for a steady state which is perturbed from its initial state of rest. Perturbations in the velocity, temperature, concentration and volume fraction of nanoparticles are decomposed into periodic disturbances given by

$$(w', T', C', \phi') = [W(z), \Theta(z), \eta(z), \Phi(z)] \exp(st + ilx + imy), \tag{10}$$

where l and m are horizontal dimensionless wave numbers in x- and y-directions, respectively, and $s = \omega_r + i\omega_i$ is a complex quantity predicting the growth rate of perturbations.

In non-dimensional form, the equation governing the flow is obtained as

$$\begin{vmatrix} -\delta^2 & \left(1 + \frac{s\lambda}{\sigma}\right)\alpha^2 \mathrm{Ra} & \left(1 + \frac{s\lambda}{\sigma}\right)\alpha^2 \frac{\mathrm{Rs}}{\mathrm{Ln}} & \left(1 + \frac{s\lambda}{\sigma}\right)\alpha^2 N_A \mathrm{Rn} \\ 1 & -\left(\delta^2 + s\right) & -N_{TC}\delta^2 & 0 \\ \frac{1}{\varepsilon} & -\delta^2 N_{CT} & -\left(\frac{\delta^2}{\mathrm{Ln}} + \frac{s}{\sigma}\right) & 0 \\ \frac{1}{\varepsilon} & \frac{\delta^2}{\mathrm{Le}} & 0 & -\left(\frac{\delta^2}{\mathrm{Le}} + \frac{s}{\sigma}\right) \end{vmatrix} = 0, \tag{11}$$

where $\delta^2 = \pi^2 + \alpha^2$,

2.1 Analysis

In this section, the marginal state of the system is discussed. The locus which separates the two classes of states as the stationary state and the oscillatory state defines the state of marginal stability of the system. The marginal state is mathematically characterized by assuming $\omega_r = 0$.

2.1.1 Stationary convection

At the marginal state ($\omega_r = 0$), if we put $\omega_i = 0$, the convection is called the stationary convection. Thermal Rayleigh number for stationary convection is obtained as

$$\mathrm{Ra}^{\mathrm{st}} = \frac{\varepsilon\left(1 - \mathrm{Ln}N_{\mathrm{TC}}N_{\mathrm{CT}}\right)\delta^4 - \mathrm{Rn}N_{\mathrm{A}}\alpha^2\left\{\varepsilon + \mathrm{Le} - \mathrm{Ln}N_{\mathrm{TC}}\left(1 + \mathrm{Le}N_{\mathrm{CT}}\right)\right\} - \mathrm{Rs}\alpha^2\left(1 - \varepsilon N_{\mathrm{CT}}\right)}{\alpha^2\left(\varepsilon - \mathrm{Ln}N_{\mathrm{TC}}\right)}. \tag{12}$$

It provides the critical Rayleigh number as

$$\mathrm{Ra}^{\mathrm{st}}_{\mathrm{cr}} = \frac{4\pi^2\varepsilon\left(1 - \mathrm{Ln}N_{\mathrm{TC}}N_{\mathrm{CT}}\right) - \mathrm{Rn}N_{\mathrm{A}}\left\{\varepsilon + \mathrm{Le} - \mathrm{Ln}N_{\mathrm{TC}}\left(1 + \mathrm{Le}N_{\mathrm{CT}}\right)\right\} - \mathrm{Rs}\left(1 - \varepsilon N_{\mathrm{CT}}\right)}{\left(\varepsilon - \mathrm{Ln}N_{\mathrm{TC}}\right)}, \tag{13}$$

where $\alpha = \pi$ is the critical wave number.

In Eq. (12), if Rn = 0, $N_{\mathrm{A}} = 0$ and Le = 0, we get a Rayleigh number for a thermosolutal convection of a fluid without nanoparticles. It is observed that if it is soluted from below (Rs > 0), the result given by Chand and Rana [45] and, for being soluted from above (Rs < 0), the result by Narayana et al. [43] are recovered.

In the absence of Dufour parameter (N_{TC}=0), Eq. (13) provides

$$\mathrm{Ra}^{\mathrm{st}} = 4\pi^2 - \mathrm{Rn}N_{\mathrm{A}}\left(1 + \frac{\mathrm{Le}}{\varepsilon}\right) - \frac{\mathrm{Rs}}{\varepsilon}(1 - \varepsilon N_{\mathrm{CT}}), \tag{14}$$

which is the same as obtained by Singh et al. [46],

which further reduces to

$$\mathrm{Ra}^{\mathrm{st}} = 4\pi^2 - \mathrm{Rn}N_{\mathrm{A}}\left(1 + \frac{\mathrm{Le}}{\varepsilon}\right) - \frac{\mathrm{Rs}}{\varepsilon} \tag{15}$$

for no Soret effect (N_{CT}=0) presented in the system, which is a critical Rayleigh number discussed by Jaimala et al. [47].

For monodiffusive convection, Eq. (16) gives a critical Rayleigh number:

$$\mathrm{Ra}^{\mathrm{st}} = 4\pi^2 - \mathrm{Rn}N_{\mathrm{A}}\left(1 + \frac{\mathrm{Le}}{\varepsilon}\right), \tag{16}$$

which is in confirmation with the one obtained by Jaimala et al. [48].

It is clear that for a system soluted from below, salt becomes a cause of earlier convection. The numerical analysis of Eq. (14) predicts that though the presence of thermo-diffusion suppresses the convection produced by the salt still double-diffusion convection occurs earlier than the monodiffusion convection.

2.1.2 Oscillatory convection

At the marginal state if $\omega_i \neq 0$, the perturbations decay or grow in oscillatory mode. The corresponding Rayleigh number is obtained as

$$\mathrm{Ra}^{\mathrm{osc}} = \frac{\sigma}{\alpha^2}\left[\frac{\left(X_1 + X_2 + X_3\right)U + \omega^2\left(Y_1 + Y_2 + Y_3\right)V}{U^2 + V^2}\right], \tag{17}$$

where

$$X_1 = \alpha^2\mathrm{Rn}N_{\mathrm{A}}\left[\delta^4\sigma^2\left\{\varepsilon + \mathrm{Le} - N_{\mathrm{TC}}\mathrm{Ln}\left(1 + \mathrm{Le}N_{\mathrm{CT}}\right)\right\} - \lambda\delta^2\omega^2(\sigma\mathrm{Le} + \varepsilon\mathrm{Ln} + \mathrm{LnLe}) - \omega^2\sigma\mathrm{LeLn}\right],$$

$$X_2 = \delta^4\varepsilon\left[\delta^4\sigma^2\left(\mathrm{Ln}N_{\mathrm{CT}}N_{\mathrm{TC}} - 1\right) - \omega^2\{\mathrm{Ln}\sigma + \mathrm{Le}\sigma + \mathrm{LeLn}\}\right],$$

$$X_3 = \alpha^2\mathrm{Rs}\left[\delta^4\sigma^2\left(1 - N_{\mathrm{CT}}\varepsilon\right) - \omega^2\left\{\lambda\delta^2\left(\sigma - \varepsilon\mathrm{Le}N_{\mathrm{CT}} + \mathrm{Le}\right) + \mathrm{Le}\sigma\right\}\right],$$

$$Y_1 = \alpha^2\mathrm{Rn}N_{\mathrm{A}}\left[\sigma\delta^2\left\langle\lambda\delta^2\left\{\varepsilon + \mathrm{Le} - N_{\mathrm{TC}}\mathrm{Ln}\left(1 + \mathrm{Le}N_{\mathrm{CT}}\right)\right\} + (\sigma\mathrm{Le} + \varepsilon\mathrm{Ln} + \mathrm{LeLn})\right\rangle - \lambda\omega^2\mathrm{LeLn}\right],$$

$$Y_2 = \varepsilon\delta^2\left[\delta^4\sigma\left(\mathrm{Ln} + \sigma - \mathrm{Le} + \mathrm{LnLe}N_{\mathrm{TC}}N_{\mathrm{CT}}\right) - \omega^2\mathrm{LeLn}\right],$$

$$Y_3 = \alpha^2\mathrm{Rs}\left\{\delta^2\sigma\left(\mathrm{Le} - \varepsilon N_{\mathrm{CT}}\mathrm{Le} + 1\right) + \lambda\delta^2\left(1 - \varepsilon N_{\mathrm{CT}}\right) - \lambda\omega^2\mathrm{Le}\right\},$$

$$U = \left[\delta^4\sigma^3\left(N_{\mathrm{TC}}\mathrm{Ln} - \varepsilon\right) + \omega^2\sigma\left\{\lambda\delta^2\left(\mathrm{Le}\varepsilon + \mathrm{Ln}\varepsilon - \mathrm{LeLn}N_{\mathrm{TC}}\right) + \varepsilon\mathrm{LeLn}\right\}\right],$$

$$V = \left[\lambda\omega^2\varepsilon\mathrm{LnLe} + \delta^2\sigma^2\left(N_{\mathrm{TC}}\mathrm{Ln}\lambda\delta^2 + N_{\mathrm{TC}}\mathrm{LeLn} - \varepsilon\mathrm{Le} - \varepsilon\lambda\delta^2 - \varepsilon\mathrm{Ln}\right)\right].$$

Here, ω_i is replaced by ω for convenience.

The frequency of oscillations ω is given by the following fourth-order equation:

$$(P_1P_2 + P_3P_4)\omega^4 + (P_1P_5 + P_2P_6 + P_3P_7 + P_4P_8)\omega^2 + (P_5P_6 + P_7P_8) = 0, \tag{18}$$

where

$$P_1 = \delta^4\varepsilon(\sigma\mathrm{Ln} + \sigma\mathrm{Le} + \mathrm{LeLn}) - \alpha^2\mathrm{Rn}N_{\mathrm{A}}\left\{\sigma\mathrm{LeLn} + \lambda\delta^2(\sigma\mathrm{Le} + \varepsilon\mathrm{Ln} + \mathrm{LeLn})\right\} - \alpha^2\mathrm{Rs}\left\{\lambda\delta^2\left(\mathrm{Le} + \sigma - \mathrm{Le}N_{\mathrm{CT}}\varepsilon\right) + \sigma\mathrm{Le}\right\},$$

$$P_2 = -\lambda\varepsilon \mathrm{LeLn},$$

$$P_3 = \mathrm{Le}\left[\delta^2\varepsilon\mathrm{Ln} - \alpha^2\lambda\left(\mathrm{Rn}N_\mathrm{A}\mathrm{Ln} - \mathrm{Rs}\right)\right],$$

$$P_4 = \sigma\left\{\delta^2\lambda\left(\varepsilon\mathrm{Le} + \varepsilon\mathrm{Ln} - \mathrm{LeLn}N_\mathrm{TC}\right) + \varepsilon\mathrm{LeLn}\right\},$$

$$P_5 = \delta^2\sigma^2\left(\lambda\delta^2 + \mathrm{Le}\right)\left(N_\mathrm{TC}\mathrm{Ln} - \varepsilon\right),$$

$$P_6 = -\delta^6\varepsilon\sigma^2\left(1 + \mathrm{Ln}N_\mathrm{CT}N_\mathrm{TC}\right) + \alpha^2\delta^4\sigma \left\langle\left\{\mathrm{Rn}N_\mathrm{A}\sigma\left[\varepsilon + \mathrm{Le} - N_\mathrm{TC}\mathrm{Ln}\left(1 + \mathrm{Le}N_\mathrm{CT}\right)\right]\right\} + \mathrm{RsLn}\left(1 - N_\mathrm{CT}\varepsilon\right)\right\rangle,$$

$$P_7 = \delta^4\sigma^3\left(N_\mathrm{TC}\mathrm{Ln} - \varepsilon\right),$$

$$P_8 = \delta^2\sigma\left[\begin{array}{l}\alpha^2\mathrm{Rn}N_\mathrm{A}\left\{\delta^4\lambda\sigma\left(\varepsilon + \mathrm{Le} - N_\mathrm{TC}\mathrm{Ln}\left(1 + \mathrm{Le}N_\mathrm{CT}\right)\right) + \sigma\mathrm{Le} + \varepsilon\mathrm{Ln} + \mathrm{LeLn}\right\} \\ -\delta^4\varepsilon\left\{\sigma\delta^2(\sigma + \mathrm{Le} + \mathrm{Ln}) + \mathrm{LnLe}N_\mathrm{CT}N_\mathrm{TC}\right\} + \alpha^2\mathrm{Rs}\left\{\sigma\mathrm{Ln}\delta^2\left(1 - N_\mathrm{CT}\varepsilon\right)\left(\mathrm{Le} + \delta^2\lambda\right) + \sigma\mathrm{Ln}\delta^2\right\}\end{array}\right].$$

3 Nonlinear stability analysis

To get the information about the amplitude of motion and the behaviour of heat, salt and mass transfer, nonlinear stability theory is implemented and we obtain the non-dimensional eigenvalue problem in the form of stream function $(u = \partial\psi/\partial z, w = -\partial\psi/\partial x)$ as

$$\nabla_1^2\psi = \left(1 + \frac{\lambda}{\sigma}\frac{\partial}{\partial t}\right)\left[-\mathrm{Ra}\frac{\partial T}{\partial x} + \mathrm{Rn}\frac{\partial\phi}{\partial x} - \frac{\mathrm{Rs}}{\mathrm{Ln}}\frac{\partial C}{\partial x}\right], \tag{19}$$

$$\frac{\partial T}{\partial t} + \frac{\partial\psi}{\partial x} = \nabla_1^2 T + \frac{\partial(\psi, T)}{\partial(x, z)} + N_\mathrm{TC}\nabla_1^2 C, \tag{20}$$

$$\frac{1}{\sigma}\frac{\partial C}{\partial t} + \frac{1}{\varepsilon}\left(\frac{\partial\psi}{\partial x}\right) = \frac{1}{\mathrm{Ln}}\nabla_1^2 C + \frac{1}{\varepsilon}\frac{\partial(\psi, C)}{\partial(x, z)} + N_\mathrm{CT}\nabla_1^2 T, \tag{21}$$

$$\frac{1}{\sigma}\frac{\partial\phi}{\partial t} - \frac{N_\mathrm{A}}{\varepsilon}\left(\frac{\partial\psi}{\partial x}\right) = \frac{1}{\mathrm{Le}}\nabla_1^2\phi + \frac{N_\mathrm{A}}{\mathrm{Le}}\nabla_1^2 T + \frac{1}{\varepsilon}\frac{\partial(\psi, \phi)}{\partial(x, z)}. \tag{22}$$

$$\psi = \frac{\partial^2\psi}{\partial z^2} = 0,\ T = 0,\ C = 0,\ \frac{\partial\phi}{\partial z} + N_\mathrm{A}\frac{\partial T}{\partial z} = 0 \text{ at } z = 0, 1. \tag{23}$$

Following Singh et al. [46], nonlinear stability analysis is performed using the Fourier expansion method. ψ, T, C and ϕ are assumed as

$$\psi = A_{11}(t)\sin(\alpha x)\sin(\pi z), \tag{24}$$

$$T = B_{11}(t)\cos(\alpha x)\sin(\pi z) + B_{02}(t)\sin(2\pi z), \tag{25}$$

$$\phi = -N_\mathrm{A}C_{11}(t)\cos(\alpha x)\sin(\pi z) - N_\mathrm{A}C_{02}(t)\sin(2\pi z), \tag{26}$$

$$C = D_{11}(t)\cos(\alpha x)\sin(\pi z) + D_{02}(t)\sin(2\pi z), \tag{27}$$

where $A_{11}(t)$, $B_{11}(t)$, $B_{02}(t)$, $C_{11}(t)$, $C_{02}(t)$, $D_{11}(t)$ and $D_{02}(t)$ are time-dependent amplitudes of the system obtained as

$$A_{11} = -\frac{\alpha}{\delta^2}\left[\mathrm{Ra}B_{11} + \mathrm{Rn}N_\mathrm{A}C_{11} + \frac{\mathrm{Rs}}{\mathrm{Ln}}D_{11} + \frac{\lambda}{\sigma}\frac{\mathrm{d}B_{11}}{\mathrm{d}t}\mathrm{Ra} + \frac{\lambda}{\sigma}\frac{\mathrm{d}C_{11}}{\mathrm{d}t}\mathrm{Rn}N_\mathrm{A} + \frac{\lambda}{\sigma}\frac{\mathrm{d}D_{11}}{\mathrm{d}t}\frac{\mathrm{Rs}}{\mathrm{Ln}}\right], \tag{28}$$

$$\frac{\mathrm{d}B_{11}}{\mathrm{d}t} = -\left[\delta^2 B_{11} + \alpha A_{11} + \pi\alpha A_{11}B_{02} + \delta^2 D_{11}N_\mathrm{TC}\right], \tag{29}$$

$$\frac{\mathrm{d}B_{02}}{\mathrm{d}t} = \frac{1}{2}\left[\pi\alpha A_{11}B_{11} - 8\pi^2\left(B_{02} + D_{02}N_\mathrm{TC}\right)\right], \tag{30}$$

$$\frac{\mathrm{d}C_{11}}{\mathrm{d}t} = -\frac{\sigma}{\varepsilon}\left[\pi\alpha A_{11}C_{02} + \alpha A_{11} + \frac{\delta^2}{\mathrm{Le}}\left(C_{11} - B_{11}\right)\right], \tag{31}$$

$$\frac{\mathrm{d}C_{02}}{\mathrm{d}t} = \frac{\sigma}{2\varepsilon}\left[\pi\alpha A_{11}C_{11} - \frac{8\pi^2}{\mathrm{Le}}\left(C_{02} - B_{02}\right)\right], \tag{32}$$

$$\frac{\mathrm{d}D_{11}}{\mathrm{d}t} = -\frac{\sigma}{\varepsilon}\left[\frac{\pi\alpha}{\varepsilon}A_{11}D_{02} + \frac{\alpha}{\varepsilon}A_{11} + \frac{\delta^2}{\mathrm{Ln}}D_{11} + \delta^2 N_\mathrm{CT}B_{11}\right], \tag{33}$$

$$\frac{\mathrm{d}D_{02}}{\mathrm{d}t} = \frac{\sigma}{2\varepsilon}\left[\frac{\pi\alpha}{\varepsilon}A_{11}D_{11} - 8\pi^2\left(\frac{D_{02}}{\mathrm{Ln}} + B_{02}N_\mathrm{CT}\right)\right]. \tag{34}$$

Equations (28)–(34) represent a nonlinear autonomous system of simultaneous ordinary differential equations. For the unsteady state, the equations are solved numerically using the Runge–Kutta–Gill method. The steady state is characterized by

$$B_{11} = \frac{\alpha A_{11}}{Y}\left[\alpha^2 x N_{TC} N_{CT} + \frac{N_{TC}\left\{\alpha^2 x \mathrm{Ln}^2(Y+Q\varepsilon) - \delta^2\varepsilon \mathrm{Ln}\right\}\left\{\delta^2 N_{CT}\varepsilon Z - \alpha^2 x \mathrm{Ln} N_{CT}(Y+Q\varepsilon) - YZ\right\}}{\left\{\alpha^2 x \mathrm{Ln}^2\left(Y^2+2YQ\varepsilon+Q^2\varepsilon^2\right) + \delta^2\varepsilon^2 Z^2\right\}} - 1\right], \tag{35}$$

$$B_{02} = \frac{\alpha^2 x}{\pi Y}\left[1 - \frac{\delta^2}{Z}\mathrm{Ln} N_{CT} N_{TC} - N_{TC}\delta^2 \mathrm{Ln}(\mathrm{Ln}Y + \mathrm{Ln}Q\varepsilon + \varepsilon Z)\left\{\frac{\delta^2 N_{CT}\varepsilon Z - \alpha^2 x \mathrm{Ln} N_{CT}(Y+Q\varepsilon) - YZ}{\alpha^2 x \mathrm{Ln}^2\left(Y^2+2YQ\varepsilon+Q^2\varepsilon^2\right) + \delta^2\varepsilon^2 Z^2}\right\}\right], \tag{36}$$

$$\begin{aligned} C_{11} = {} & \frac{\varepsilon\alpha A_{11}}{\left\{\delta^2\varepsilon^2 + \alpha^2 x \mathrm{Le}^2\right\} YZ}\left[\alpha^2 x \mathrm{Ln}Q(\mathrm{Le}+\varepsilon) - \delta^2(\mathrm{Le}+\varepsilon)Z\right] \\ & + \frac{\alpha A_{11}\varepsilon \mathrm{Ln}}{\left\{\delta^2\varepsilon^2 + \alpha^2 x \mathrm{Le}^2\right\} YZ}\left[\varepsilon Z\left(\alpha^2 x \mathrm{Le} - \delta^2\varepsilon\right) + \alpha^2 x \mathrm{Ln}Y(\mathrm{Le}+\varepsilon)\right] \\ & \times \left[\frac{\delta^2 N_{CT}\varepsilon Z - \alpha^2 x \mathrm{Ln} N_{CT}(Y+Q\varepsilon) - YZ}{\alpha^2 x \mathrm{Ln}^2\left(Y^2+2YQ\varepsilon+Q^2\varepsilon^2\right) + \delta^2\varepsilon^2 Z^2}\right], \end{aligned} \tag{37}$$

$$\begin{aligned} C_{02} = {} & \frac{\alpha^2 x \mathrm{Le}}{\left\{\delta^2\varepsilon^2 + \alpha^2 x \mathrm{Le}^2\right\} YZ}\left[\alpha^2 x \mathrm{Ln}Q(\mathrm{Le}+\varepsilon) - \delta^2(\mathrm{Le}+\varepsilon)Z\right] + \frac{\alpha^2 x \mathrm{Ln}\mathrm{Le}}{\left\{\delta^2\varepsilon^2 + \alpha^2 x \mathrm{Le}^2\right\} YZ} \\ & \times \left[\varepsilon Z\left(\alpha^2 x \mathrm{Le} - \delta^2\varepsilon\right) + \alpha^2 x \mathrm{Ln}Y(\mathrm{Le}+\varepsilon)\right]\left[\frac{\delta^2 N_{CT}\varepsilon Z - \alpha^2 x \mathrm{Ln} N_{CT}(Y+Q\varepsilon) - YZ}{\alpha^2 x \mathrm{Ln}^2\left(Y^2+2YQ\varepsilon+Q^2\varepsilon^2\right) + \delta^2\varepsilon^2 Z^2}\right] \\ & + \frac{\alpha^2 x}{\pi Y}\left[1 - \frac{\delta^2}{Z}\mathrm{Ln} N_{CT} N_{TC} - N_{TC}\delta^2 \mathrm{Ln}(\mathrm{Ln}Y + \mathrm{Ln}Q\varepsilon + \varepsilon Z)\left\{\frac{\delta^2 N_{CT}\varepsilon Z - \alpha^2 x \mathrm{Ln} N_{CT}(Y+Q\varepsilon) - YZ}{\alpha^2 x \mathrm{Ln}^2\left(Y^2+2YQ\varepsilon+Q^2\varepsilon^2\right) + \delta^2\varepsilon^2 Z^2}\right\}\right], \end{aligned} \tag{38}$$

$$D_{11} = \alpha A_{11}\varepsilon \mathrm{Ln}\left[\frac{\delta^2 N_{CT}\varepsilon Z - \alpha^2 x \mathrm{Ln} N_{CT}(Y+Q\varepsilon) - YZ}{\alpha^2 x \mathrm{Ln}^2\left(Y^2+2YQ\varepsilon+Q^2\varepsilon^2\right) + \delta^2\varepsilon^2 Z^2}\right], \tag{39}$$

$$D_{02} = \frac{\alpha^2 x \mathrm{Ln}}{\pi Z}\left[N_{CT} + \mathrm{Ln}(Y+Q\varepsilon)\left\{\frac{\delta^2 N_{CT}\varepsilon Z - \alpha^2 x \mathrm{Ln} N_{CT}(Y+Q\varepsilon) - YZ}{\alpha^2 x \mathrm{Ln}^2\left(Y^2+2YQ\varepsilon+Q^2\varepsilon^2\right) + \delta^2\varepsilon^2 Z^2}\right\}\right], \tag{40}$$

where $x = \left(A_{11}^2/8\right)$, $Q = \delta^2 N_{TC} N_{CT}$, $Y = \delta^2 + \alpha^2 x$, $Z = Y - \mathrm{Ln}Q$.

3.1 Heat, salt and nanoparticles transport

The thermal Nusselt number, solutal concentration Nusselt number and nanoparticles concentration Nusselt number providing the heat, salt and nanoparticle transport, respectively, are obtained as

$$\mathrm{Nu}(t) = 1 - 2\pi B_{02}(t), \tag{41}$$

$$\mathrm{Nu}_C(t) = 1 - 2\pi D_{02}(t) + N_{CT}\left(1 - 2\pi B_{02}(t)\right), \tag{42}$$

$$\mathrm{Nu}_\phi(t) = 1 + 2\pi\left(B_{02}(t) - C_{02}(t)\right). \tag{43}$$

It is clear that the heat, salt and nanoparticles are transferred through diffusion as well as convection governed by the Soret as well as Dufour effect.

4 Results and discussion

A comparison of the stationary convection with the one for a Darcy–Maxwell fluid without nanoparticles [45] is made in Fig. 2. It is clear that for specified values of the parameters Rs = 5, Le = 10, Rn = 0.5, $\varepsilon = 0.4$, Ln = 10, $N_A = 1$, $N_{CT} = 0.1$ and $N_{TC} = 0.01$, the presence of nanoparticles enhances the convection, which is physically realistic due to the Brownian motion.

Figure 3 represents a comparison of the convections in monodiffusion, double diffusion, diffusion with Soret effect and diffusion in the presence of both the Soret and Dufour effects. The graphs confirm that the salt sets the convection earlier which is delayed to some extent if Soret effect is also present but not to the level of monodiffusion convection. It is clear that among the four types of convections the critical Rayleigh number is maximum for the convection with cross-diffusion effects, indicating that the simultaneous presence of Soret and Dufour parameters enhances the stability by delaying the convection.

In Fig. 4a–c, we draw the linear stability curves for thermosolutal Lewis number, Soret parameter and Dufour parameter by varying one of the parameters and assigning fixed values to other relevant parameters.

On taking the thermosolutal Lewis number Ln > 1, the diffusion of heat is more than the diffusion of salt and on

increment of Ln; hence, Fig. 4a shows that as the thermosolutal Lewis number increases the Rayleigh number also increases that makes the system stable. Notably, the dual behaviour of the parameter in a regular Maxwell fluid [45] changes to stabilizing parameter in a nanofluid. Figure 4b, c exposes the effects of Soret parameter and Dufour parameter, respectively. It can be seen that Soret parameter still has a dual character as it has for a fluid without nanoparticles [45], but the dual behaviour of Dufour parameter N_{TC} does not persist in the presence of nanoparticles and converts to an agent bringing the stability to the system.

Marginal state oscillatory convection is portrayed through Fig. 5a–j. The graphs are drawn for fixed values $\mathrm{Rn} = 0.1$, $\mathrm{Rs} = 2$, $\mathrm{Le} = 10$, $\varepsilon = 0.5, \mathrm{Ln} = 10, N_A = 2$, $N_{CT} = 1.1$, $N_{TC} = 0.1$, $\lambda = 0.01$ and $\sigma = 0.8$ with variations in one of the parameters. Clearly, the parameters Rs, Rn, ε, N_A, λ and N_{CT} hasten the onset of convection and also to enlarge the size of convection cells (Fig. 5a, b, d, f, h, i), while Fig. 5c, e, g illustrates the dual nature of thermo-nanofluid Lewis number Le, the thermosolutal Lewis number Ln and σ. The effect of Dufour parameter N_{TC} is illustrated in Fig. 5j proving it to be the stabilizing agent for oscillatory convection.

For the steady state, Fig. 6a–h describes the comparison of the rate of transfer of heat, salt and nanoparticles together with their individual behaviour with respect to different parameters. It is to be noticed that independent of the behaviour of any parameter, the rate of transfer of heat is the lowest, while the salt is transferred at the highest rate. Comparing the transfer of heat with that in a regular fluid [41], it is seen that it is increased in the presence of nanoparticles. The result is also true on physical grounds as nanoparticles are proved to enhance thermal conductivity of the fluid. It is also observed that for large values of Rayleigh number, the transfer of heat, salt and mass attains a constant rate. In Fig. 6a, the effect of solutal Rayleigh number Rs is shown. It is clear that as Rs increases, Nu_C and Nu_ϕ increase, but Nu decreases. Thus, the parameter Rs enhances the salt transfer and mass transfer but suppresses the heat transfer. The same behaviour is observed for the parameters Rn and N_A (Fig. 6b, c). The behaviour of the parameters ε, Ln, N_{TC}, Le and N_{CT} is shown in Fig. 6d–h. As ε increases, the transfer of heat is increased, but it decreases the transfer of mass and salt. Ln and N_{TC} enhance the transfer of heat and salt but decrease the transfer of mass. Figure 6g illustrates that Le is responsible to enhance the transfer of heat and mass while the transfer of salt is suppressed. From Fig. 6h, we find that on increasing the Soret parameter N_{CT}, the transfer of salt is increased, while the transfer of heat and nanoparticles is decreased.

Figure 7 shows the time-independent patterns of ψ, T, ϕ and C at different values of Ra. It is observed that the strength of streamlines increases with greater Ra (Fig. 7a, b). The streamlines move alternately identical in the subsequent cells but move in the directions opposite to each other. It indicates the symmetrical formation of the

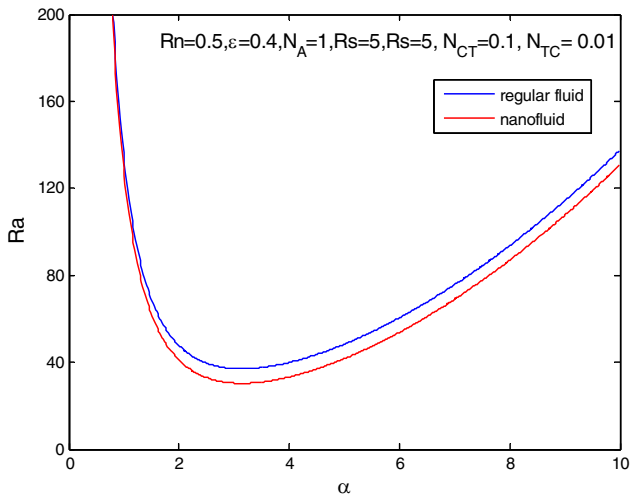

Fig. 2 A comparison of convections in regular fluid and nanofluid

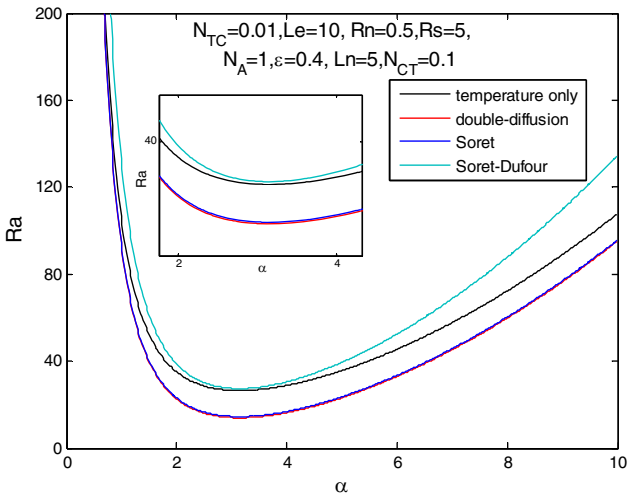

Fig. 3 A comparison in monodiffusion, double diffusion, thermo-diffusion and cross-diffusion

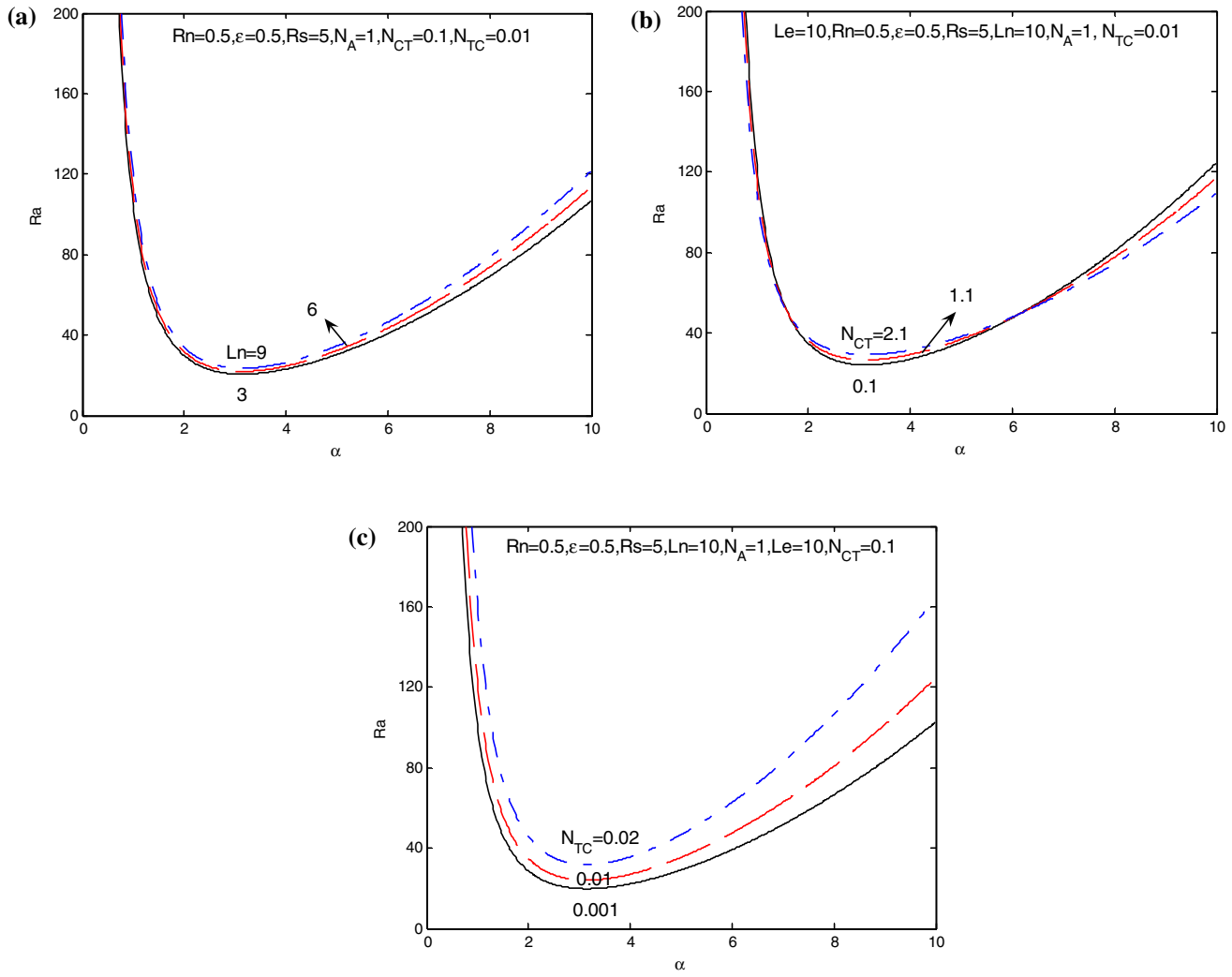

Fig. 4 Linear stationary convection for **a** Ln, **b** N_{CT}, **c** N_{TC}

convective cells. It is seen that as Ra increases the convective mode of heat transfer becomes stronger (Fig. 7c, d). Similarly, the isonanoconcentrations and isohalines occur in slightly increased form with increased Ra (Fig. 7e–h).

In the unsteady state of motion, the transient behaviour of Nu, Nu_C and Nu_ϕ is plotted with respect to time for given values of $Rn = 4, \varepsilon = 0.4, Rs = 5, Ln = 10, N_A = 2, Le = 10, \sigma = 0.8, \lambda = 0.5, N_{CT} = 0.1, N_{TC} = 0.01$ by varying any one of these parameters. It is observed that initially ($t = 0$) heat, salt and mass are transferred at a high rate through conduction/diffusion and then attaining vigorous oscillations for a while these approach to a stationary state. Figure 8b, f, g predicts that on increasing Rn, N_A and σ, transfer of heat is suppressed, while it is enhanced for ε (Fig. 8d). Since thermo-nanofluid Lewis number Le is the ratio of thermal to Brownian coefficient; hence, on increasing its value it results in weaker Brownian diffusivity which simply represents lower nanoparticle concentration [15]. On taking $Le > 1$, it enhances the amount heat transfer (Fig. 8c).

Figure 9 shows that none of the parameters except the Dufour parameter N_{TC} has a significant effect on the transfer of salt. N_{TC} initially increases the salt transport but after a certain time transport is decayed and attains a constant value.

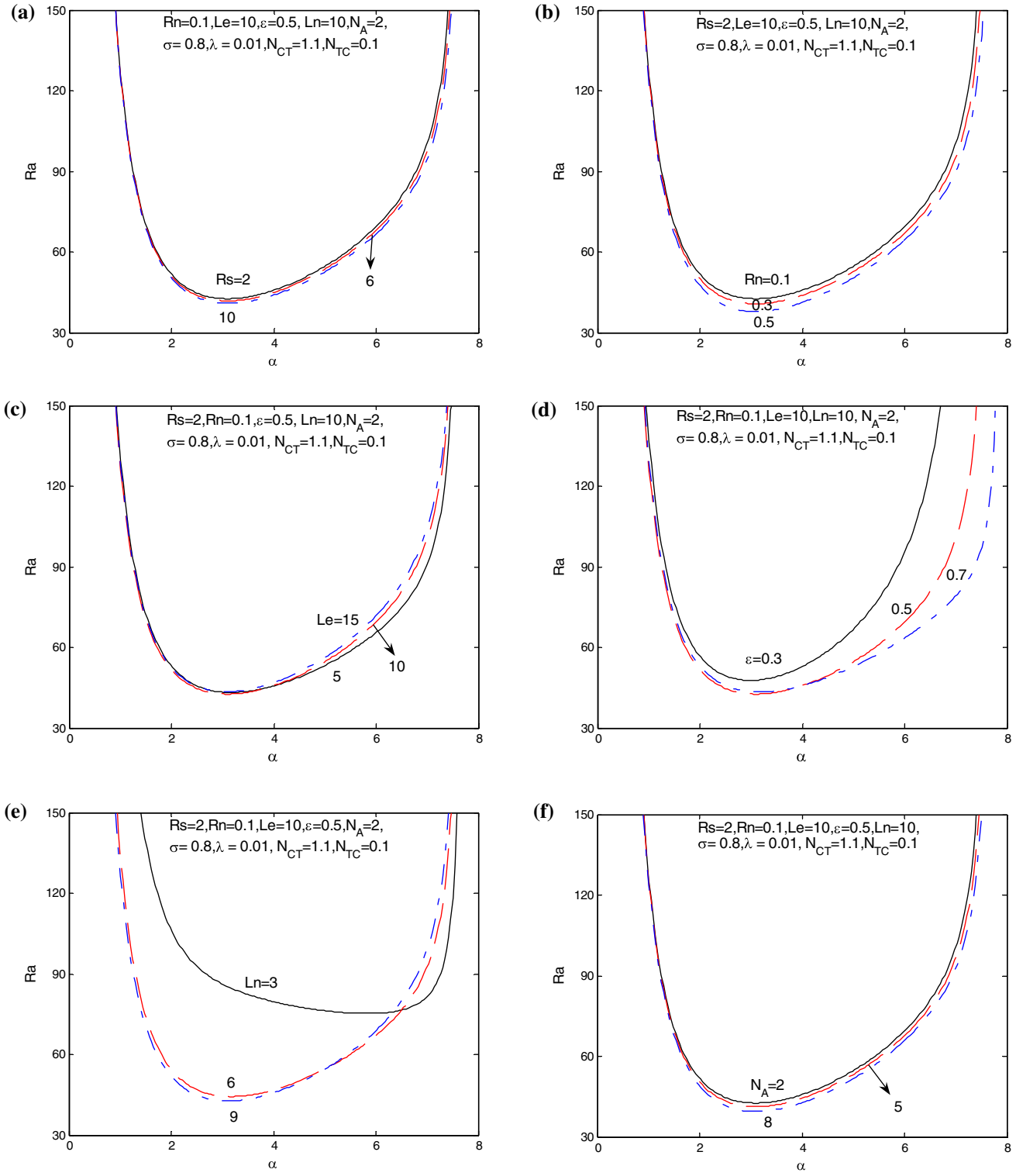

Fig. 5 Linear oscillatory convection for **a** Rs, **b** Rn, **c** Le, **d** ε, **e** Ln, **f** N_A, **g** σ, **h** λ, **i** N_{CT}, **j** N_{TC}

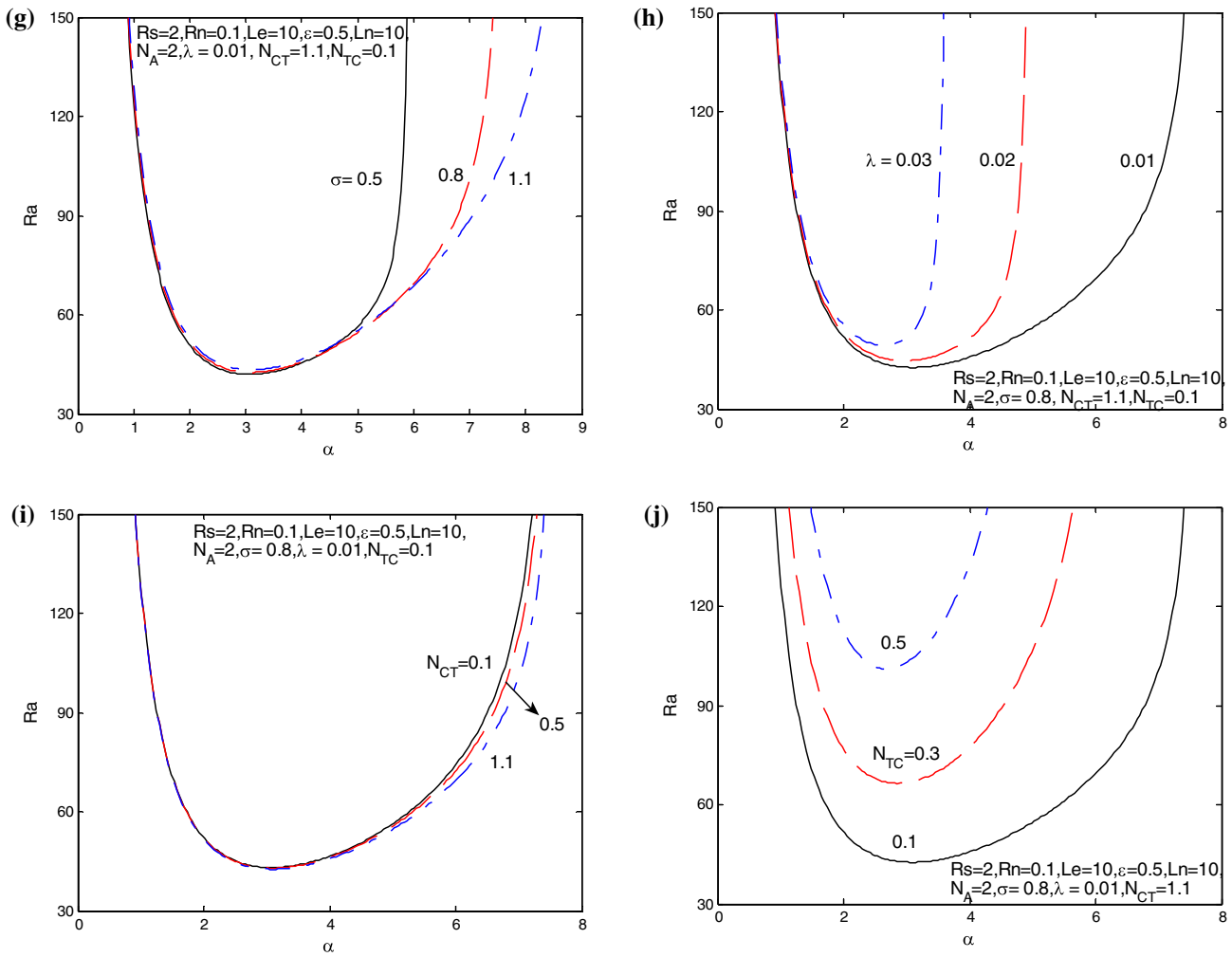

Fig. 5 (continued)

Figure 10 states that the transfer of nanoparticles is not affected by changing any of the parameters, concluding that the presence of salt together with cross-diffusion effect does not change the pattern and amount of the transfer of nanoparticles.

Graphs for the streamlines, isotherms, isonanoconcentrations and isohalines for the given values of Rn= 4, $\varepsilon = 0.4$, Rs= 5, Ln= 10, $N_A = 2$, $\sigma = 0.8$, $\lambda = 0.5$, Le= 10, $N_{CT} = 0.1$ and $N_{TC} = 0.01$ at two different times, $t = 0.02$ and $t = 2$, are shown in Fig. 11. It is to be noted from Fig. 11a, b that the same symmetrical formation of the convective cells of motion of streamlines is formed in a steady case, but the strength of stream function reduces with time. Figure 11c, d predicts that with the time the convective mode of heat transfer becomes weak and conduction is seen in the middle of layers. Figure 11e, f shows that the mass of nanoparticles initially transfers through strong convection, but with the time it loses its evenness and strong diffusion occurs. The same type of behaviour is noticed for the transfer of salt (Fig. 11g, h).

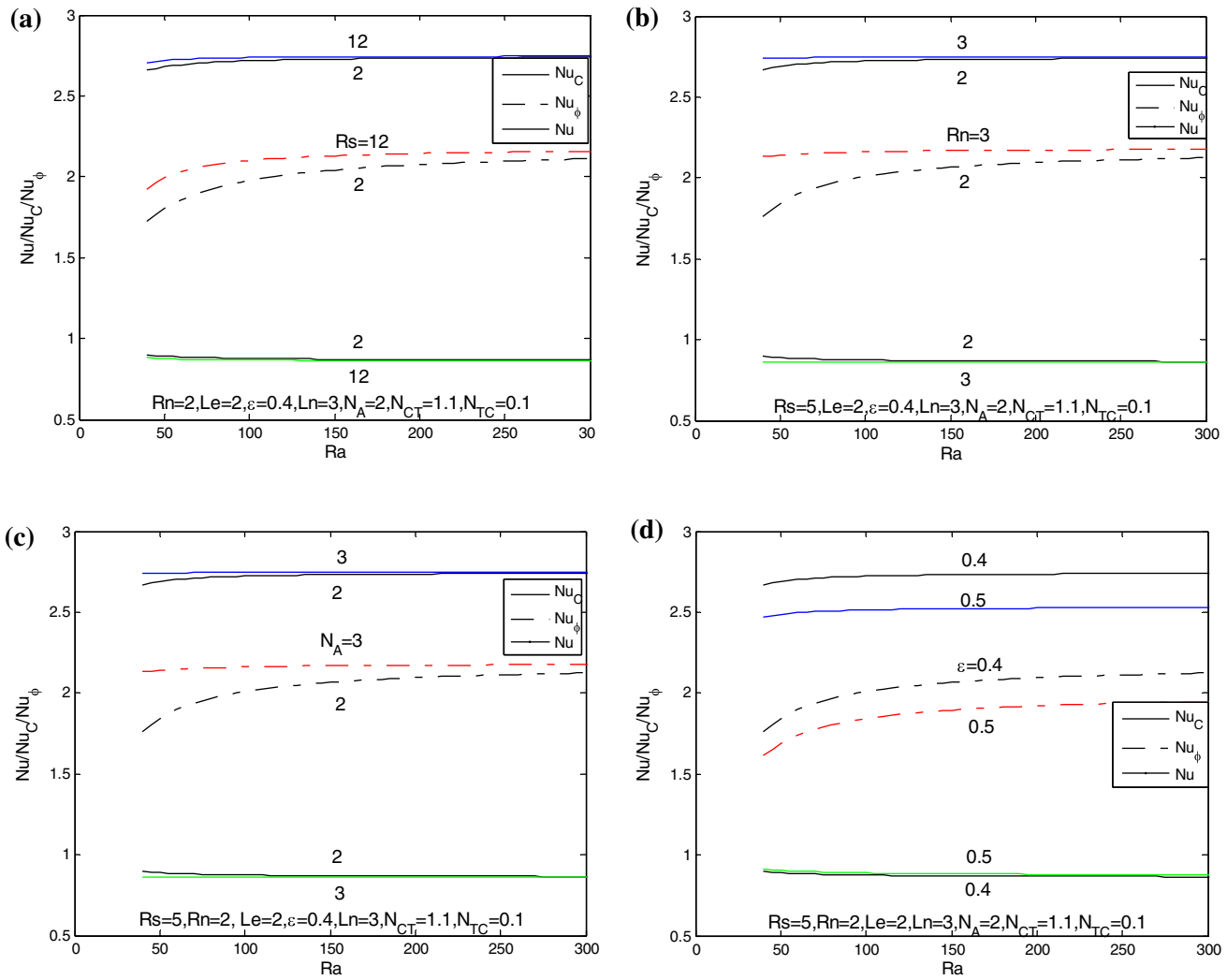

Fig. 6 Nu,Nu_C and Nu_ϕ in the steady state for **a** Rs, **b** Rn, **c** N_A, **d** Le, **e** N_{TC}, **f** ε, **g** Ln, **h** N_{CT}

5 Conclusion

The cross-diffusion effects in a Darcy porous layer saturated with a binary viscoelastic Maxwell nanofluid have been investigated numerically and graphically. It is observed that the stationary convection is supported and enhanced by the presence of nanoparticles. The stability of the stationary convection is maintained by the porosity, the thermosolutal Lewis number and the Soret and Dufour parameters, while the parameters Rs, Rn, Le and N_A interrupt the stability and advance the convection. Further, it is noted that though nanoparticles advance the stationary convection it is suppressed by the presence of cross-diffusion effects. Oscillatory convection is enhanced by the parameters Rs, Rn, ε, Ln, N_A and N_{CT}, but Le, λ and N_{TC} suppress it. A dual effect of the parameter σ is observed. Initially, it delays the convection up to a certain value of α, but beyond that it advances the convection.

The nonlinear theory predicts that in comparison with the heat and nanoparticles, transfer of salt is maximum. The parameters ε, Ln, N_{CT} and Le increase the transfer of heat, whereas the parameters Rs, Rn, N_A and N_{TC} decrease

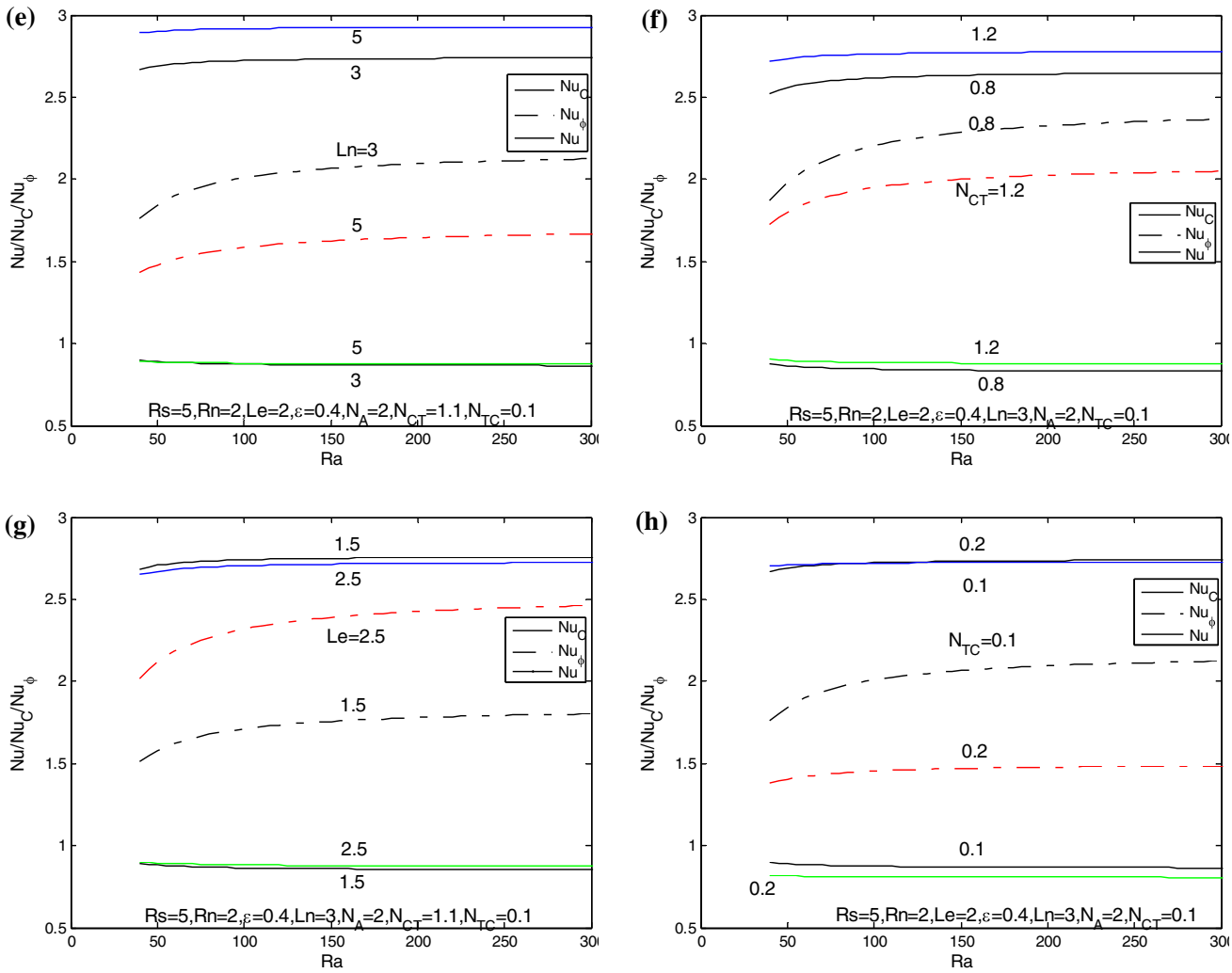

Fig. 6 (continued)

it. Rs, Rn and N_A are responsible for increasing the transfer of salt and nanoparticles. Ln enhances the transfer of salt but delays the transfer of nanoparticles. Le supports the mass transfer and opposes the salt transfer. The parameters N_{CT} and N_{TC} slow down the speed of the transfer of mass and enhance the salt transfer. The porosity parameter ε opposes the transfer of salt and nanoparticles.

In the steady state, the magnitude of stream function increases with an increased Ra, while in the unsteady state it is decreased with time. Isotherms, isonanoconcentrations and isohalines occur completely in the form of convection in the steady state. In the unsteady motion, convective mode of transfer of salt and nanoparticle concentrations completely changes to conduction/diffusion mode as the time passes.

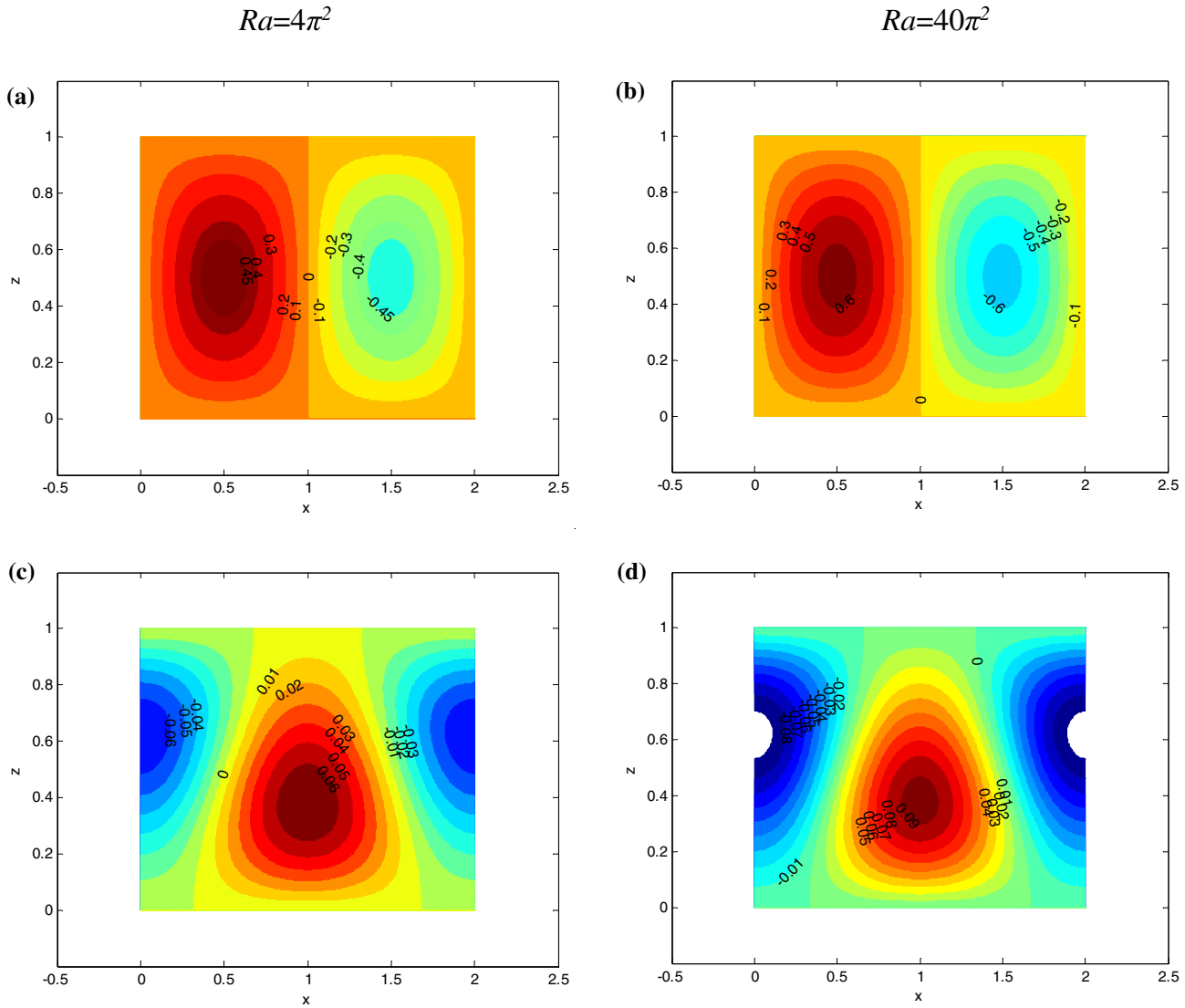

Fig. 7 Streamlines, isotherms, isonanoconcentration and isohalines for Rs = 5; Rn = 4; Le = 10; ε = 0.4; Ln = 10; $N_A = 2$; $N_{CT} = 0.1$; $N_{TC} = 0.01$

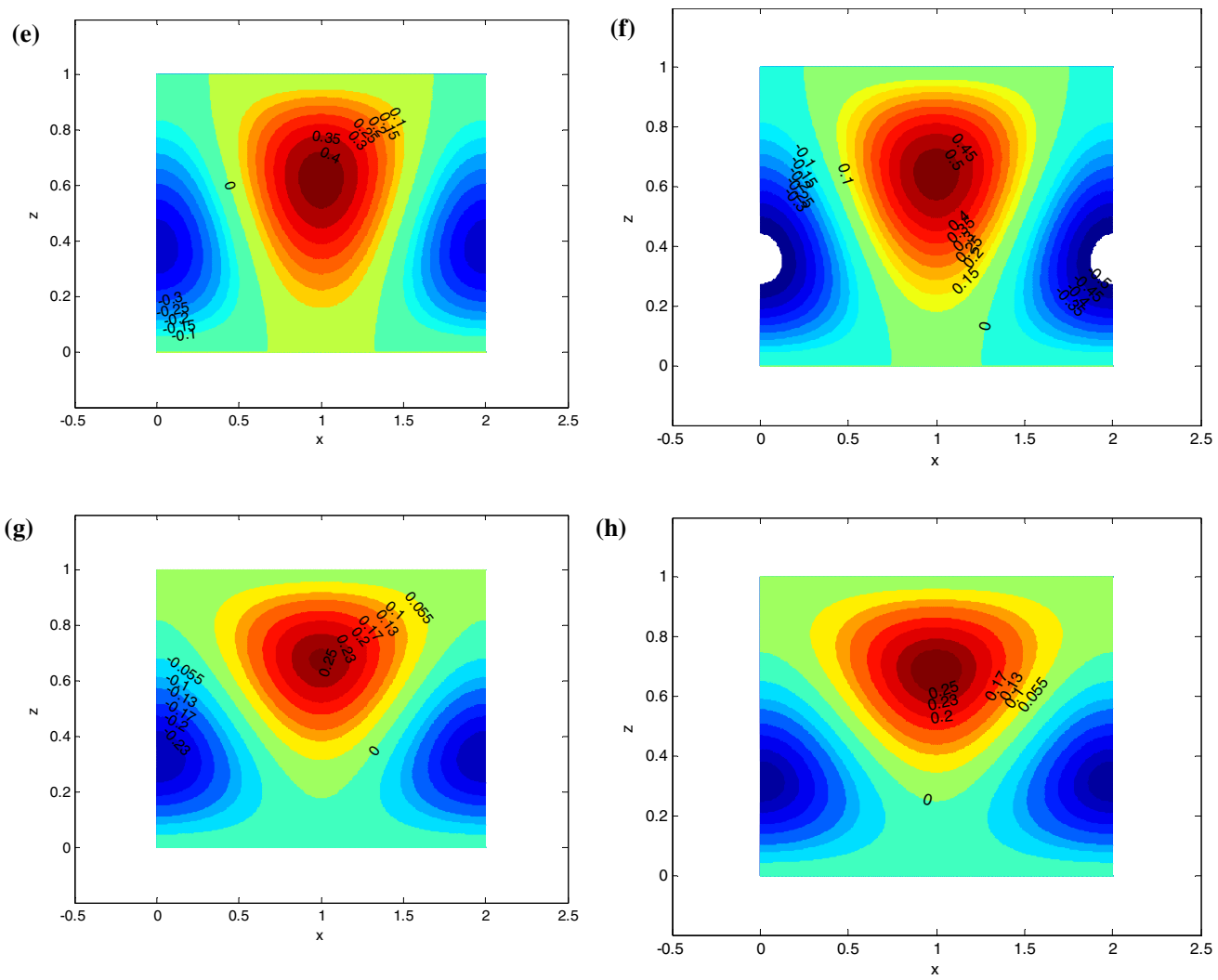

Fig. 7 (continued)

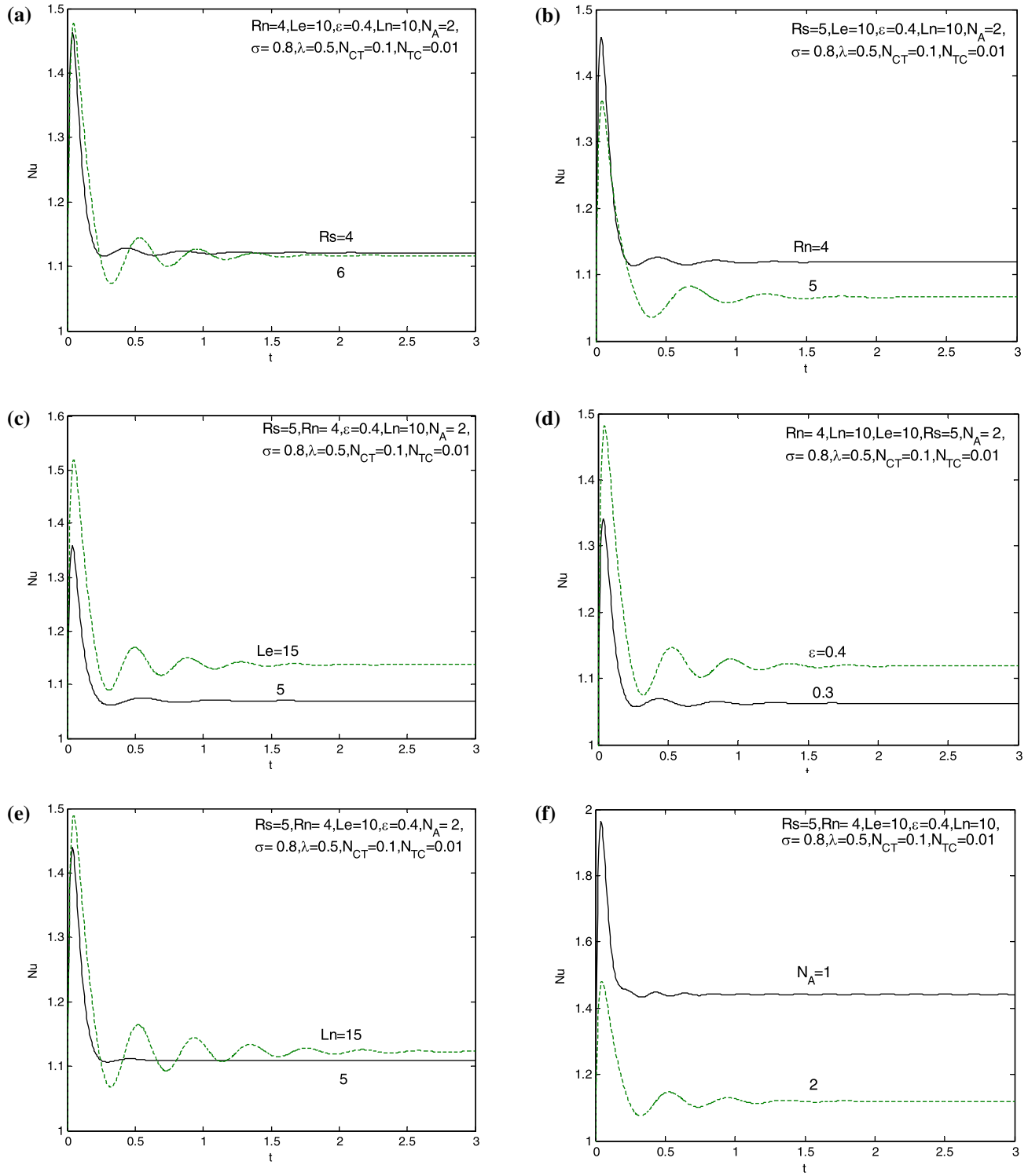

Fig. 8 Nu versus *t* for **a** Rs, **b** Rn, **c** Le, **d** ε, **e** Ln, **f** N_A, **g** σ, **h** λ, **i** N_{CT}, **j** N_{TC}

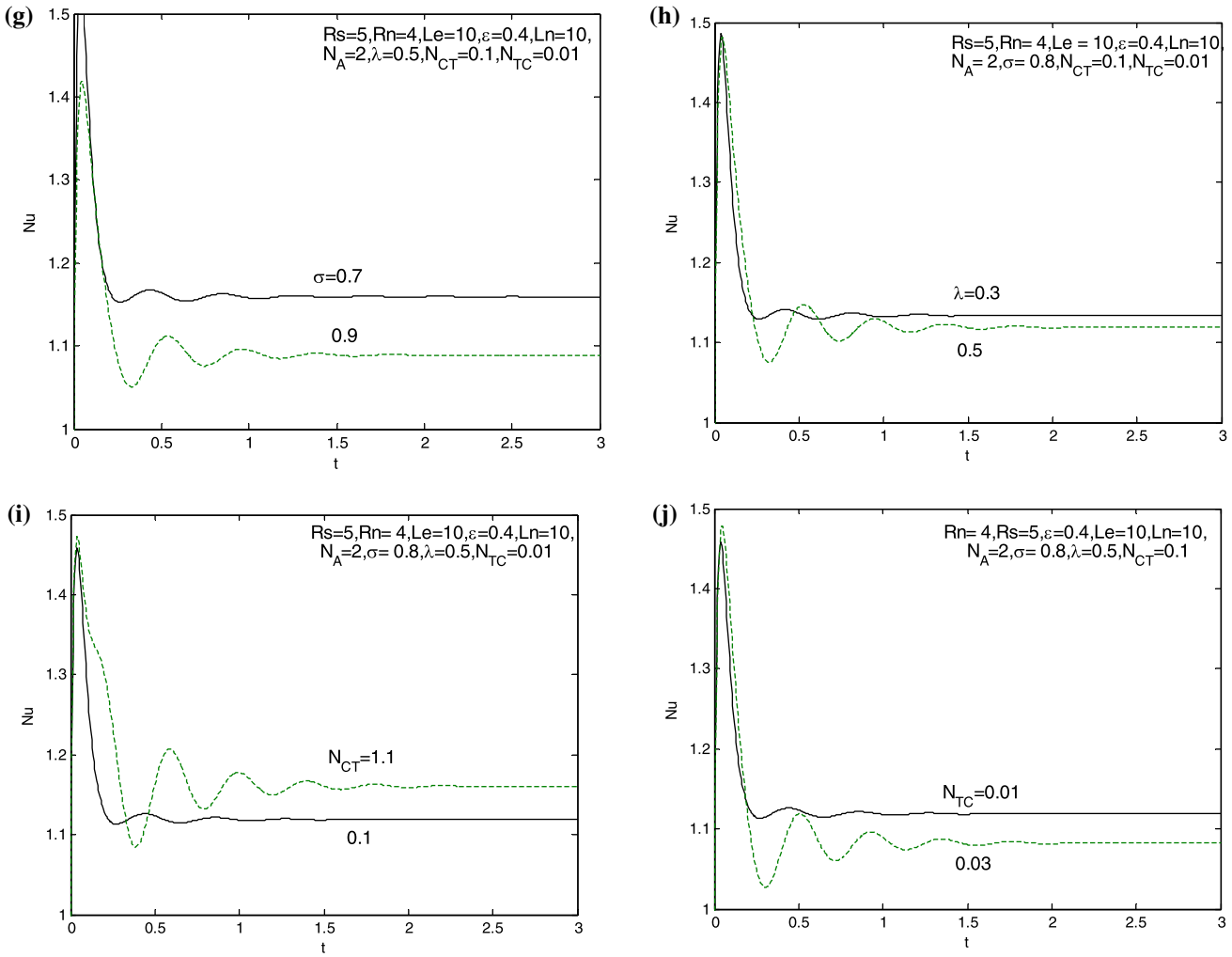

Fig. 8 (continued)

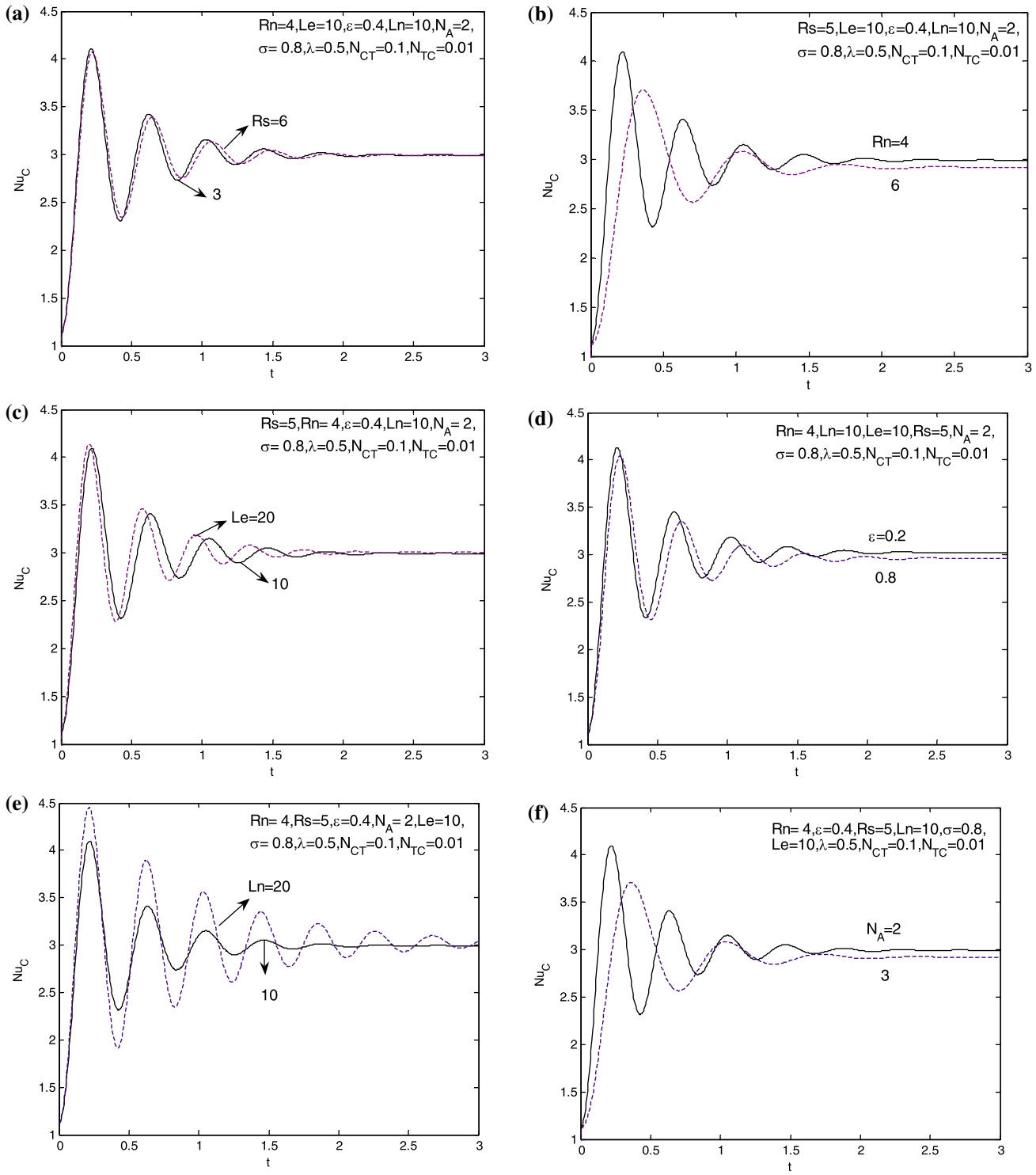

Fig. 9 Nu_C versus t for **a** Rs, **b** Rn, **c** Le, **d** ε, **e** Ln, **f** N_A, **g** σ, **h** λ, **i** N_{CT}, **j** N_{TC}

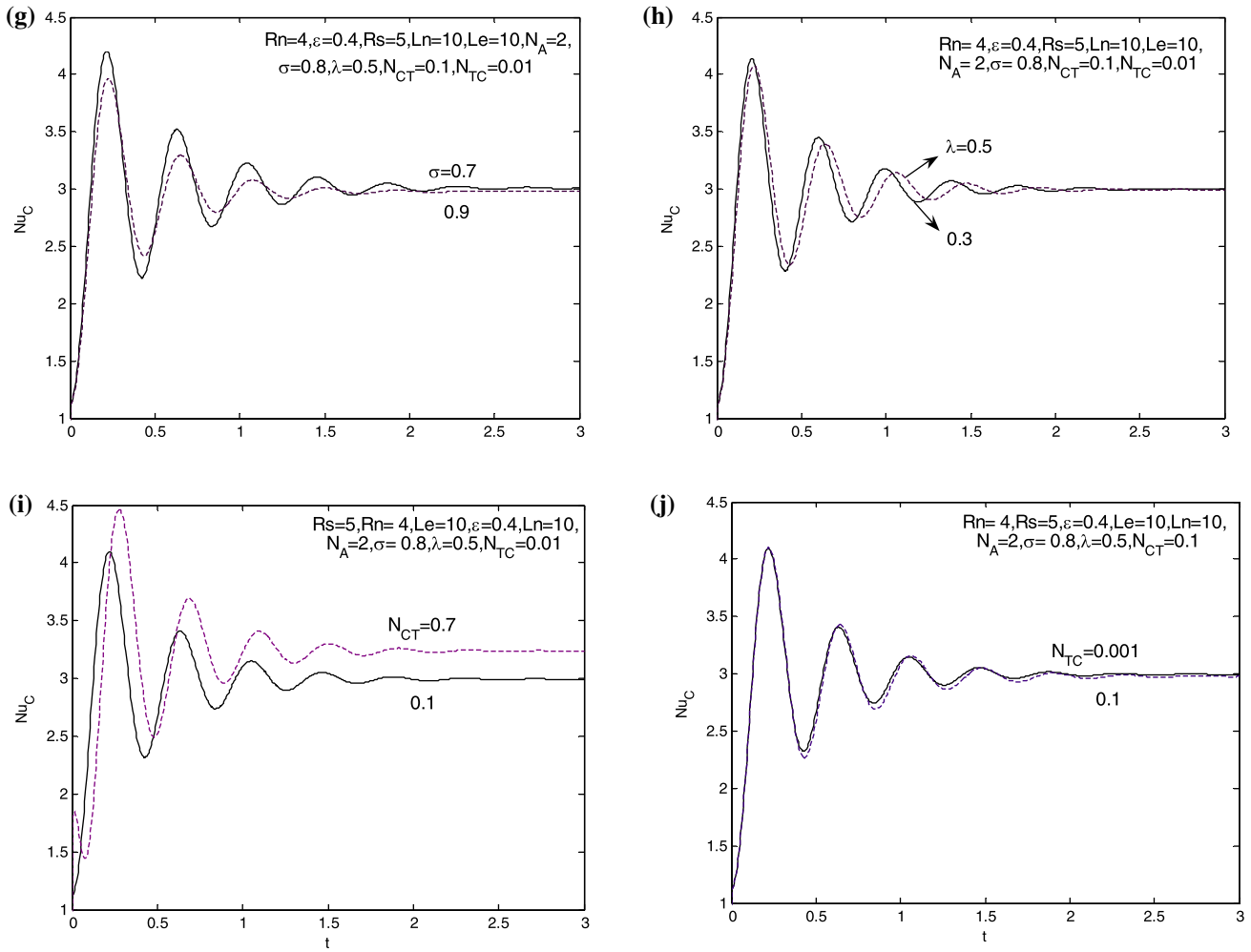

Fig. 9 (continued)

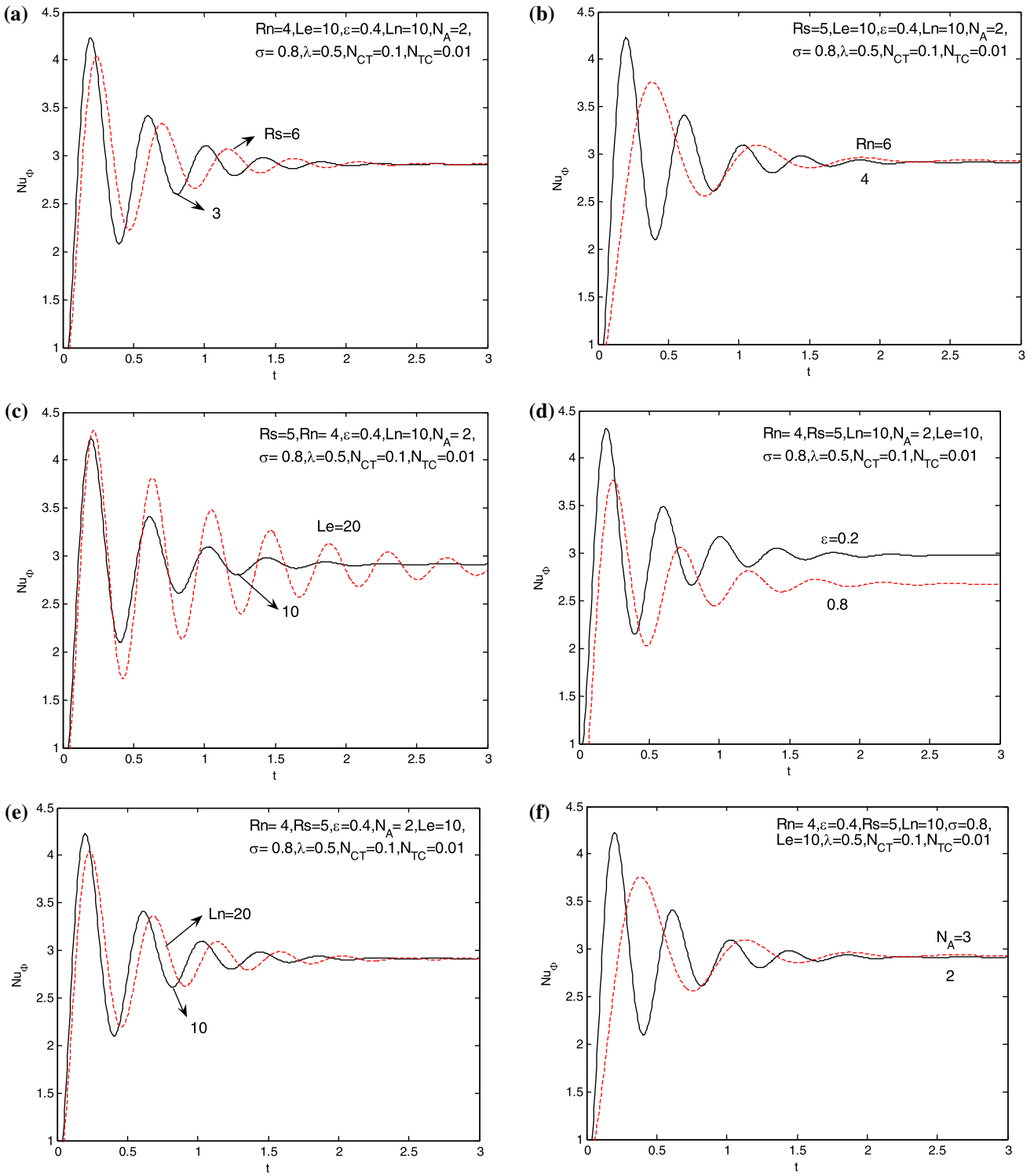

Fig. 10 Nu_{ϕ} versus t for **a** Rs, **b** Rn, **c** Le, **d** ε, **e** Ln, **f** N_A, **g** σ, **h** λ, **i** N_{CT}, **j** N_{TC}

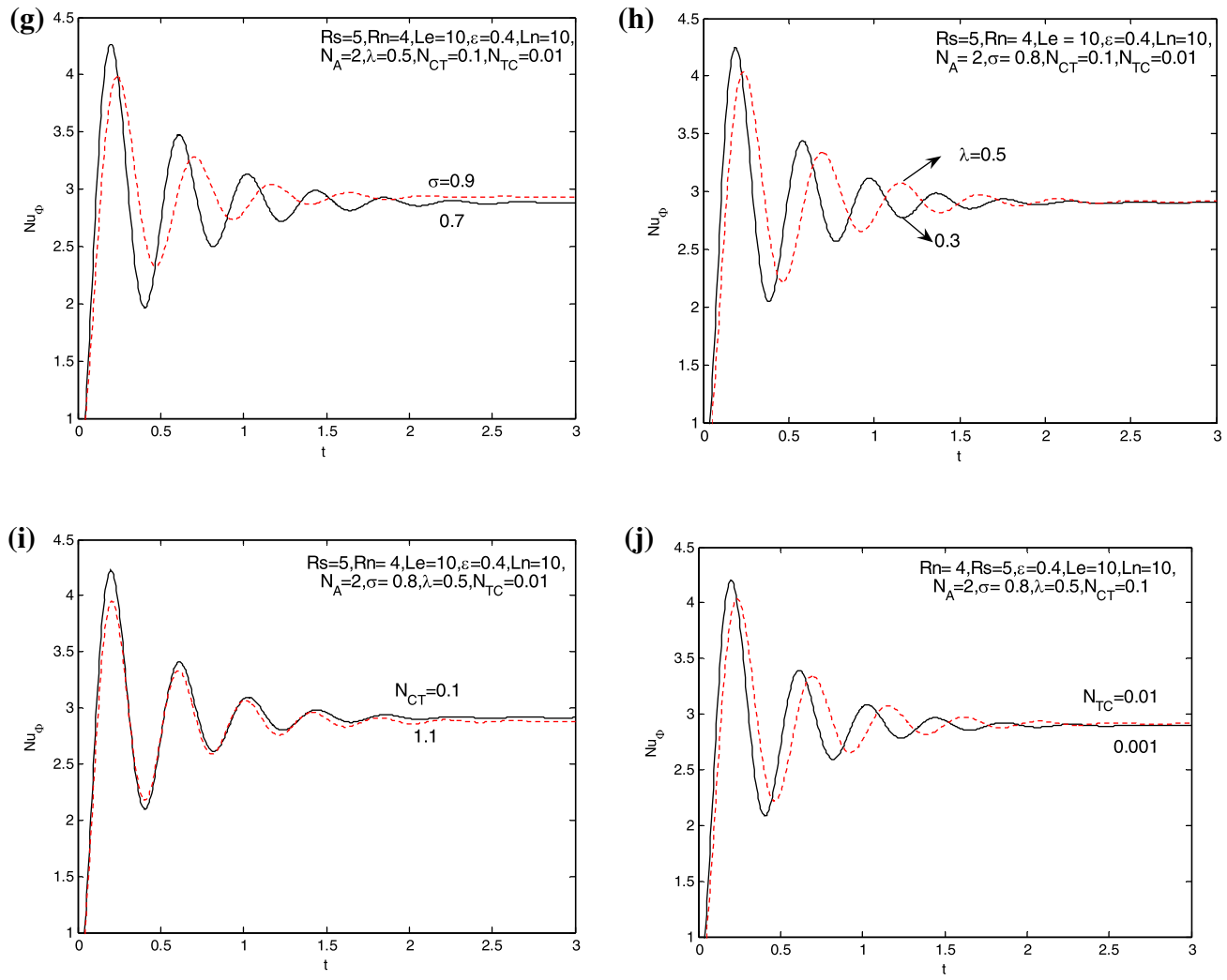

Fig. 10 (continued)

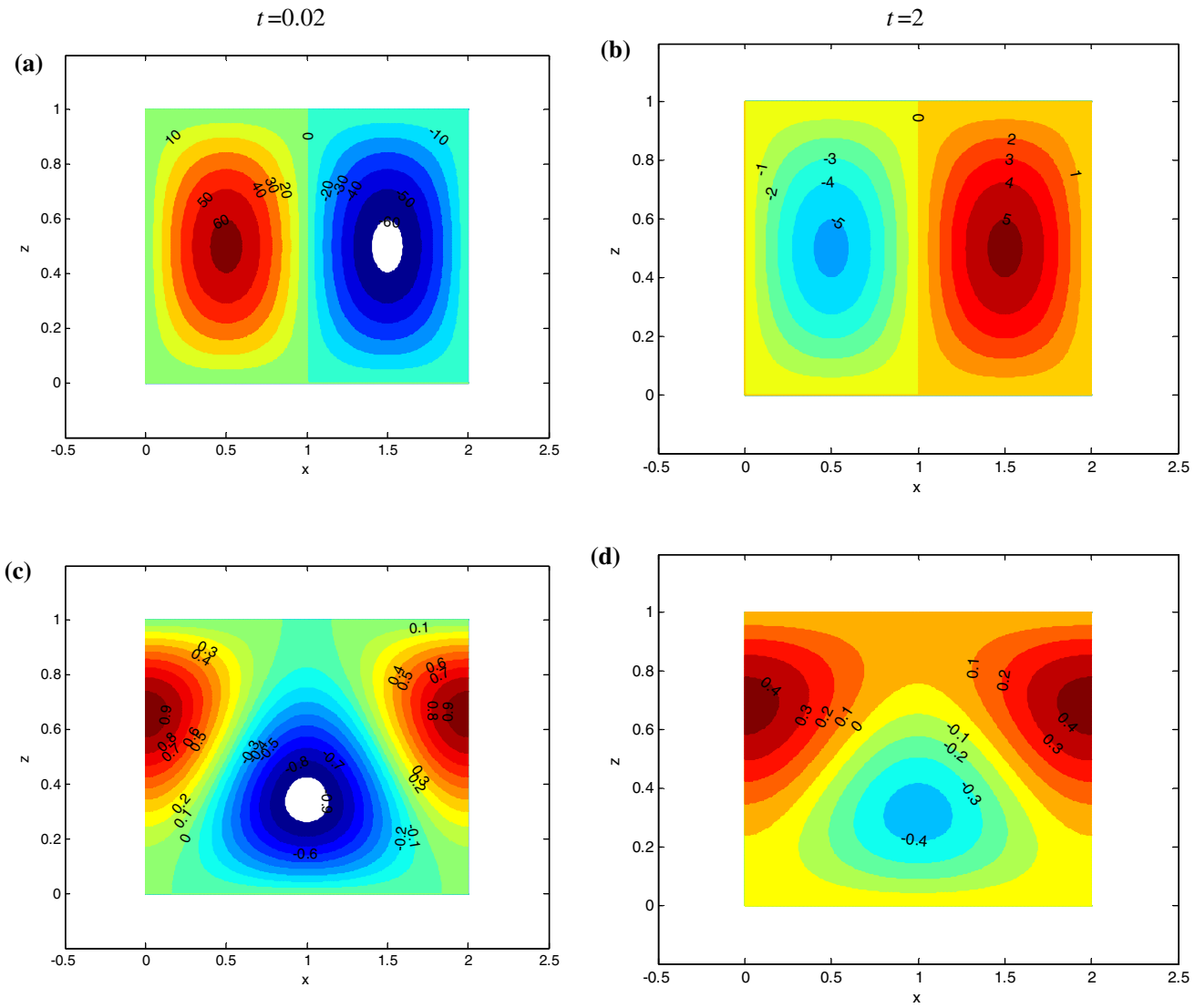

Fig. 11 Streamlines, isotherms, isonanoconcentration and isohalines in the unsteady state

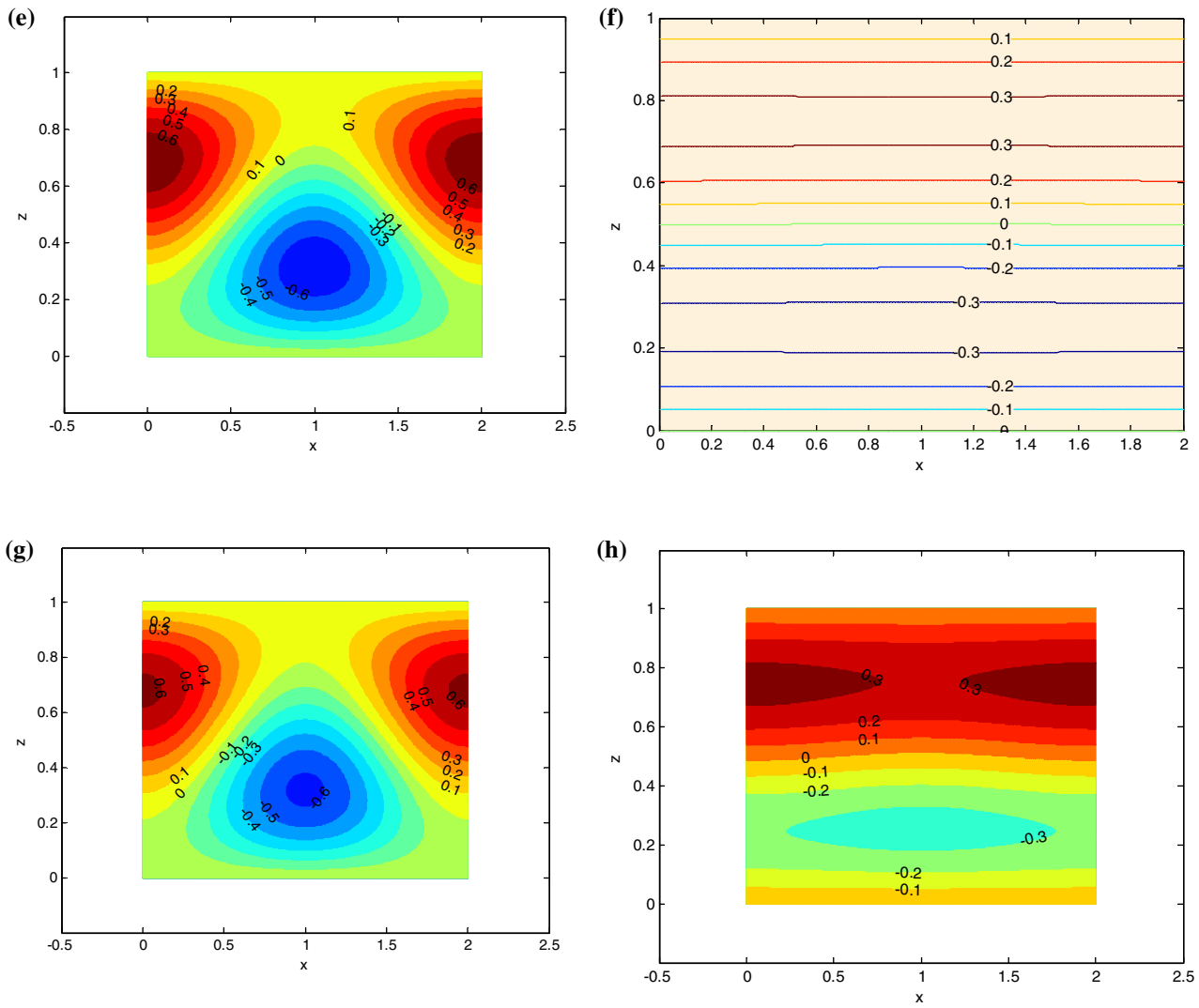

Fig. 11 (continued)

Acknowledgements The authors wish to gratefully acknowledge financial support through major research Project No. F. 42-9/2013 (SR) from the University Grants Commission (UGC), New Delhi.

Compliance with ethical standards

Conflict of interest The authors declare that they have no conflict of interest.

References

1. Alishayev MG (1974) Proceedings of Moscow Pedagogy Institute. Hydromechanics 3:166–174
2. Eastman JA, Phillpot SR, Choi SUS, Keblinski P (2004) Thermal transport in nanofluids. Annu Rev Mater Res 34(1):219–246. https://doi.org/10.1146/annurev.matsci.34.052803.090621
3. Das SK, Choi SUS, Wenhua Y, Pradeep T (2007) Nanofluids: science and technology. Wiley, New York
4. Bianco V, Manca O, Nardini S, Vafai K (2015) Heat transfer enhancement with nanofluids. CRC Press, Boca Raton
5. Nield DA, Bejan A (2017) Convection in porous media, 5th edn. Springer, New York
6. Choi SUS, Cho YI, Kasza KE (1992) Degradation effects of dilute polymer solutions on turbulent friction and heat transfer behaviour. J Non-Newtonian Fluid Mech 41(3):289–307. https://doi.org/10.1016/0377-0257(92)87003-T
7. Buongiorno J (2006) Convective transport in nanofluids. ASME J Heat Transf 128(3):240–250. https://doi.org/10.1115/1.2150834

8. RamReddy Ch, Murthy PVSN, Chamkha Ali J, Rashad AM (2013) Soret effect on mixed convection flow in a nanofluid under convective boundary condition. Int J Heat Mass Transf 64:384–392. https://doi.org/10.1016/j.ijheatmasstransfer.2013.04.032
9. Mehryan SAM, Kashkooli Farshad M, Mohammad Ghalambaz, Chamkha Ali J (2017) Free convection of hybrid Al_2O_3-Cu water nanofluid in a differentially heated porous cavity. Adv Powder Technol 28(9):2295–2305. https://doi.org/10.1016/j.apt.2017.06.011
10. Chamkha Ali J, Maysam Molana, Ali Rahnama, Ghadami F (2018) On the nanofluids applications in microchannels: a comprehensive review. Powder Technol 332(1):287–322. https://doi.org/10.1016/j.powtec.2018.03.044
11. Reddy Gorla Rama Subba, Chamkha Ali J (2011) Natural convective boundary layer flow over a nonisothermal vertical plate embedded in a porous medium saturated with a nanofluid. Nanosc Microsc Therm 15:81–94. https://doi.org/10.1080/15567265.2010.549931
12. Chamkha Ali J, Abbasbandy S, Rashad AM, Vajravelu K (2013) Radiation effects on mixed convection about a cone embedded in a porous medium filled with a nanofluid. Meccanica 48:275–285. https://doi.org/10.1007/s11012-012-9599-1
13. Reddy PS, Chamkha Ali J (2016) Soret and Dufour effects on MHD convective flow of Al_2O_3–water and TiO_2–water nanofluids past a stretching sheet in porous media with heat generation/absorption. Adv Powder Technol 27(4):1207–1218. https://doi.org/10.1016/j.apt.2016.04.005
14. Reddy PS, Sreedevi P, Chamkha Ali J (2017) MHD boundary layer flow, heat and mass transfer analysis over a rotating disk through porous medium saturated by Cu-water and Ag-water nanofluid with chemical reaction. Powder Technol 307(1):46–55. https://doi.org/10.1016/j.powtec.2016.11.017
15. Hayat T, Aziz A, Muhammad T, Alsaedi A (2017) A revised model for Jeffrey nanofluid subject to convective condition and heat generation/absorption. PLoS ONE 12(2):e0172518. https://doi.org/10.1371/journal.pone.0172518
16. Radko T (2013) Double-diffusive convection. Cambridge University Press, Cambridge
17. Chamkha Ali J, Groşan T, Pop I (2002) Fully developed free convection of a micropolar fluid in a vertical channel. Int Commun Heat Mass Transf 29(8):1119–1127. https://doi.org/10.1016/S0735-1933(02)00440-2
18. Al-Mudhaf A, Chamkha Ali J (2005) Similarity solutions for MHD thermosolutal Marangoni convection over a flat surface in the presence of heat generation or absorption effects. Heat Mass Transf 42:112–121. https://doi.org/10.1007/s00231-004-0611-8
19. Umavathi JC, Kumar JP, Chamkha Ali J, Pop I (2005) Mixed convection in a vertical porous channel. Transp Porous Med 61:315–335. https://doi.org/10.1007/s11242-005-0260-5
20. Magyari E, Chamkha Ali J (2008) Exact analytical results for the thermosolutal MHD Marangoni boundary layers. Int J Therm Sci 47(7):848–857. https://doi.org/10.1016/j.ijthermalsci.2007.07.004
21. Khedr MEM, Chamkha Ali J, Beyomi M (2009) MHD flow of a micropolar fluid past a stretched permeable surface with heat generation or absorption. Nonlinear Anal Model 14(1):27–40. https://doi.org/10.15388/na.2009.14.1.14528
22. Magyari E, Chamkha Ali J (2010) Combined effect of heat generation or absorption and first-order chemical reaction on micropolar fluid flows over a uniformly stretched permeable surface: the full analytical solution. Int J Therm Sci 49(9):1821–1828. https://doi.org/10.1016/j.ijthermalsci.2010.04.007
23. Chamkha Ali J, Mohamed RA, Ahmed Sameh E (2011) Unsteady MHD natural convection from a heated vertical porous plate in a micropolar fluid with Joule heating, chemical reaction and radiation effects. Meccanica 46:399–411. https://doi.org/10.1007/s11012-010-9321-0
24. Dufour L (1873) Poggend Ann Physik 148:490
25. Ingle SE, Horne FH (1973) The Dufour effect. J Chem Phys 59(11):5882. https://doi.org/10.1063/1.1679957
26. Soret Ch (1879) Sur l'état d'équilibre que prend, au point de vue de sa concentration, une dissolution saline primitivement homogène, dont deux parties sont portées à des températures différentes; Archives de Genève, 3e periode. Arch Sci Phys Nat 2:48–61
27. De Groot SR, Mazur P (1962) Non-equilibrium thermodynamics. North-Holland Publishing Company, Amsterdam
28. Eckert ERG, Drake RM (1972) Analysis of heat and mass transfer. McGraw-Hill, New York
29. Nithyadevi N, Yang RJ (2009) Double diffusive natural convection in a partially heated enclosure with Soret and Dufour effects. Int J Heat Fluid Flow 30(5):902–910. https://doi.org/10.1016/j.ijheatfluidflow.2009.04.001
30. Weaver JA, Viskanta R (1986) Freezing of liquid-saturated porous media. J Heat Transf 108(3):654–659. https://doi.org/10.1115/1.3246986
31. Ryskin A, Muller HW, Pleiner H (2003) Thermal convection in binary fluid mixtures with a weak concentration diffusivity, but strong solutal buoyancy forces. Phys Rev E Stat Nonlin Soft Matter Phys 67:046302. https://doi.org/10.1103/PhysRevE.67.046302
32. Kim J, Kang YT, Choi CK (2004) Analysis of convective instability and heat transfer characteristics of nanofluid. Phys Fluids 16:2395–2401. https://doi.org/10.1063/1.1739247
33. Kim MC, Hong JS, Choi CK (2006) The analysis of the onset of Soret-driven convection in nanoparticles suspension. Fluid Mech Transp Phenom 52:2333–2339
34. Kim MC, Choi CK (2007) Analysis of onset of Soret-driven convection by the energy method. Phys Rev E Stat Nonlin Soft Matter Phys 76:036302. https://doi.org/10.1103/PhysRevE.76.036302
35. Baehr HD, Stephan K (2011) Heat and mass transfer, 3rd edn. New York, Springer
36. Nield DA, Kuznetsov AV (2014) Thermal instability in a porous medium layer saturated by a nanofluid: a revised model. Int J Heat Mass Transf 68:211–214. https://doi.org/10.1016/j.ijheatmasstransfer.2013.09.026
37. Khuzhayorov B, Auriault JL, Royer P (2000) Derivation macroscopic filtration law for transient linear fluid flow in porous media. Int J Eng Sci 38(5):487–504. https://doi.org/10.1016/S0020-7225(99)00048-8
38. Wang S, Tan W (2008) Stability analysis of double-diffusive convection of Maxwell fluid in a porous medium heated from below. Phys Lett A 372(17):3046–3050. https://doi.org/10.1016/j.physleta.2008.01.024
39. Awad FG, Sibanda P, Motsa SS (2010) On the linear stability analysis of a Maxwell fluid with double-diffusive convection. Appl Math Model 34(11):3509–3517. https://doi.org/10.1016/j.apm.2010.02.038
40. Wang S, Tan W (2011) Stability analysis of Soret-driven double-diffusive convection of Maxwell fluid in a porous medium. Int J Heat Fluid Flow 32(1):88–94. https://doi.org/10.1016/j.ijheatfluidflow.2010.10.005
41. Malashetty MS, Biradar BS (2011) The onset of double diffusive convection in a binary Maxwell fluid saturated porous layer with cross-diffusion effects. Phys Fluids 23(6):064109. https://doi.org/10.1063/1.3601482
42. Jaimala Goyal N (2012) Soret Dufour driven thermosolutal instability of Darcy-Maxwell fluid. IJE Trans A Basic 25(4):367–377
43. Narayana M, Sibanda P, Motsa SS, Narayana PAL (2012) Linear and nonlinear stability analysis of binary Maxwell fluid

convection in a porous medium. Heat Mass Transf 48(5):863–874. https://doi.org/10.1007/s00231-011-0939-9
44. Zhao M, Zhang Q, Wang S (2014) Linear and nonlinear stability analysis of double diffusive convection in a Maxwell fluid saturated porous layer with internal heat source. J Appl Math. https://doi.org/10.1155/2014/489279
45. Chand R, Rana GC (2014) Double diffusive convection in a layer of Maxwell viscoelastic fluid in porous medium in the presence of Soret and Dufour effects. J Fluids. https://doi.org/10.1155/2014/479107
46. Singh R, Bishnoi J, Tyagi VK (2019) Onset of Soret driven instability in a Darcy–Maxwell nanofluid. SN Appl Sci 1(10):1–29. https://doi.org/10.1007/s42452-019-1325-3
47. Jaimala Singh R, Tyagi VK (2018) Stability of a double diffusive convection in a Darcy porous layer saturated with Maxwell nanofluid under macroscopic filtration law: a realistic approach. Int J Heat Mass Transf 125:290–309. https://doi.org/10.1016/j.ijheatmasstransfer.2018.04.070
48. Jaimala Singh R, Tyagi VK (2017) A macroscopic filtration model for natural convection in a Darcy Maxwell nanofluid saturated porous layer with no nanoparticle flux at the boundary. Int J Heat Mass Transf 111:451–466. https://doi.org/10.1016/j.ijheatmasstransfer.2017.04.003